INTERNATIONAL JOURNAL OF
NUMERICAL ANALYSIS AND MODELING
Volume 16, Number 2, Pages 167–191

AN ITERATIVE APPROACH FOR CONSTRUCTING IMMERSED FINITE ELEMENT SPACES AND APPLICATIONS TO INTERFACE PROBLEMS

CHENG WANG, PENGTAO SUN, AND ZHILIN LI

Abstract. In this paper, an iterative approach for constructing immersed finite element spaces is developed for various interface conditions of interface problems involving multiple primary variables. Combining such iteratively constructed immersed finite element spaces with the distributed Lagrange multiplier/fictitious domain (DLM/FD) method, we further present a new discretization method that can uniformly solve general interface problems with multiple primary variables and/or with different governing equations on either side of the interface, including fluid-structure interaction problems. The strengths of the proposed method are shown in the numerical experiments for Stokes- and Stokes/elliptic interface problems with different types of interface conditions, where, the optimal or nearly optimal convergence rates are obtained for the velocity variable in H^1, L^2 and L^∞ norms, and at least 1.5-th order convergence for the pressure variable in L^2 norm within few number of iterations. In addition, numerical experiments show that such iterative process uniformly converges and the number of iteration is independent of mesh ratios and jump ratios.

Key words. Immersed finite element (IFE) method, fictitious domain method, Lagrange multiplier, iterative process, interface problems, fluid-structure interactions (FSI).

1. Introduction

Physical phenomena in a domain consisting of multiple materials or fluids with an interface are often modeled by differential equations with discontinuous coefficients which are often called interface problems. Solutions to interface problems are often required to satisfy jump conditions across the material interfaces in addition to the pertinent differential equations and the related boundary conditions. In general, interface problems require the governing differential equations at the common interface to share not only the common value of primary variable (Dirichlet-type interface condition) but also the common flux (Neumann-type interface condition).

Due to its simplicity in mesh generation (one single uniform mesh usually works well), the body-unfitted mesh method becomes more promising in solving interface problems with moving interfaces possessing sophisticated and irregular shapes. Among the existing body-unfitted mesh methods, for example, the extended finite element method (XFEM), also known as a generalized finite element method (GFEM) in which enrichment functions are added near the interface [32]; unfitted discontinuous Galerkin methods with penalties [27]; unfitted finite element method based on the Nitsche's method in [15] and etc., the immersed finite element (IFE) method, which was originally proposed in [20, 21] for solving elliptic interface problems, turns out to be the most accurate and efficient because it can avoid the smearing of the sharp interface without introducing any local mesh enrichment, and maintains second-order accuracy by incorporating the known jump conditions at the interface into the finite element space.

Received by the editors July 31, 2017 and, accepted January 27, 2018.
2000 *Mathematics Subject Classification.* 65N30, 65R20.

Since its beginning, the IFE method has been mostly applied to the elliptic interface problem [21, 23, 16, 17, 1, 18, 19] due to the simplicities of both governing equation and interface conditions. However, the IFE method still suffers from applying to the Stokes interface problem because of its sophisticated governing equations (an intrinsic saddle-point structure) and complicated interface conditions in contrast with the elliptic interface problem, making the stable mixed finite element (Stokes-pair) very difficult to be defined and analyzed in the immersed finite element space. So far, only a mixed IFE Q_1/Q_0 is designed for the following Stokes interface problem (1)-(8) [2], however, the discontinuous Galerkin method has to be relied on in order to stabilize the mixed IFE Q_1/Q_0 since Q_1/Q_0 is not a stable Stokes-pair.

$$-\nabla\cdot(\beta_1\nabla\boldsymbol{u}_1)+\nabla p_1=\boldsymbol{f}_1, \qquad \text{in } \Omega_1, \tag{1}$$

$$\nabla\cdot\boldsymbol{u}_1=0, \qquad \text{in } \Omega_1, \tag{2}$$

$$-\nabla\cdot(\beta_2\nabla\boldsymbol{u}_2)+\nabla p_2=\boldsymbol{f}_2, \qquad \text{in } \Omega_2, \tag{3}$$

$$\nabla\cdot\boldsymbol{u}_2=0, \qquad \text{in } \Omega_2, \tag{4}$$

$$\boldsymbol{u}_1=\boldsymbol{u}_2, \qquad \text{on } \Gamma, \tag{5}$$

$$(\beta_1\nabla\boldsymbol{u}_1-p_1\boldsymbol{I})\boldsymbol{n}_1+(\beta_2\nabla\boldsymbol{u}_2-p_2\boldsymbol{I})\boldsymbol{n}_2=\boldsymbol{w}, \qquad \text{on } \Gamma, \tag{6}$$

$$\boldsymbol{u}_1=0, \qquad \text{on } \partial\Omega_1\backslash\Gamma, \tag{7}$$

$$\boldsymbol{u}_2=0, \qquad \text{on } \partial\Omega_2\backslash\Gamma, \tag{8}$$

where, $\Omega=\Omega_1\cup\Omega_2\subset\mathcal{R}^d$ as shown in Figure 1, and the immersed interface $\Gamma=\partial\Omega_2$ is generally a closed curve that divides the domain Ω into an interior region Ω_2 and an exterior region Ω_1, and splits an arbitrary function $\boldsymbol{\phi}\in L^2(\Omega)$ to be $\boldsymbol{\phi}|_{\Omega_i}=\boldsymbol{\phi}_i\,(i=1,2)$, where the subscripts 1 and 2 indicate the restrictions to the corresponding subdomain, $\boldsymbol{n}_1$ and $\boldsymbol{n}_2$ stand for the unit outward normal vectors on $\partial\Omega_1$ and $\partial\Omega_2$, respectively. We assume $\boldsymbol{f}_i\in\left(L^2(\Omega_i)\right)^d$, $\boldsymbol{w}\in\left(H^{1/2}(\Gamma)\right)^d$. The coefficient $\beta(\boldsymbol{x})$ and the source term $\boldsymbol{f}(\boldsymbol{x})$ may exhibit discontinuities across Γ, but have smooth restrictions $\beta_1(\boldsymbol{x})$, $\boldsymbol{f}_1(\boldsymbol{x})$ in Ω_1 and $\beta_2(\boldsymbol{x})$, $\boldsymbol{f}_2(\boldsymbol{x})$ in Ω_2. In addition, the following regularity properties are held for the Stokes interface problem (1)-(8) if the interface Γ is of class C^2 [31]

$$\boldsymbol{u}\in\boldsymbol{X}:=(H^s(\Omega))^d\cap(H^2(\Omega_1\cup\Omega_2))^d, \quad p\in\boldsymbol{Y}:=L^2(\Omega)\cap H^1(\Omega_1\cup\Omega_2), \tag{9}$$

where, $1<s<1.5$.

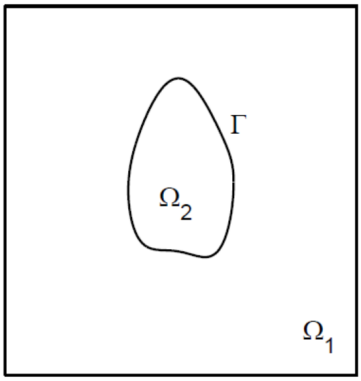

FIGURE 1. Graphical depiction of the domain with an immersed interface.

On the other hand, because IFE method needs to define the immersed finite element space by introducing interface conditions into the definition of piecewise polynomial basis functions in the interface elements which are cut through by the interface Γ, it requires that the primary variables which are involved in all interface conditions have to be defined in both sides of the interface, which is, however, impossible for interface problems whose governing equations thus primary variables on either side of the interface are different from each other, for example, the following Stokes/elliptic interface problem which is also considered as a linearized steady state fluid-structure interaction (FSI) problem, defined as

$$-\nabla\cdot(\beta_1\nabla\boldsymbol{u}_1)+\nabla p_1=\boldsymbol{f}_1, \qquad \text{in } \Omega_1, \tag{10}$$

$$\nabla\cdot\boldsymbol{u}_1=0, \qquad \text{in } \Omega_1, \tag{11}$$

$$-\nabla\cdot(\beta_2\nabla\boldsymbol{u}_2)=\boldsymbol{f}_2, \qquad \text{in } \Omega_2, \tag{12}$$

$$\boldsymbol{u}_1=\boldsymbol{u}_2, \qquad \text{on } \Gamma, \tag{13}$$

$$(\beta_1\nabla\boldsymbol{u}_1-p_1\boldsymbol{I})\boldsymbol{n}_1+\beta_2\nabla\boldsymbol{u}_2\boldsymbol{n}_2=\boldsymbol{w}, \qquad \text{on } \Gamma, \tag{14}$$

$$\boldsymbol{u}_1=0, \qquad \text{on } \partial\Omega_1\backslash\Gamma, \tag{15}$$

$$\boldsymbol{u}_2=0, \qquad \text{on } \partial\Omega_2\backslash\Gamma, \tag{16}$$

where, the vector variable $\boldsymbol{u}$ is defined in the entire domain Ω but the pressure p is only defined in Ω_1 for Stokes equations, inducing different flux forms on either side of Γ, as shown in (14). Therefore, the standard IFE P_1 space that is originally designed for the elliptic interface problem cannot be directly defined for the above Stokes/elliptic interface problem. Moreover, the IFE method cannot be directly applied to FSI problem either because the fluid equation and the structure equation are completely distinct from each other in the sense of different variables, different stress forms and even different coordinate descriptions [12, 10, 28]. By the way, with the assumption $\boldsymbol{f}_i\in\left(L^2(\Omega_i)\right)^d$, $\boldsymbol{w}\in\left(H^{1/2}(\Gamma)\right)^d$, a similar regularity result of velocity $\boldsymbol{u}$ with that of Stokes interface problem, together with the regularity of pressure p that is defined in Ω_1 only, can be assumed for the Stokes/elliptic interface problem (10)-(16) [29, Chapter 2] as follows

$$\boldsymbol{u}\in\boldsymbol{X},\quad p\in H^1(\Omega_1). \tag{17}$$

It is worthy to refer to a Cartesian finite difference-based augmented immersed interface method (AIIM) that is proposed in [24] for Navier–Stokes interface problem and in [22] for Stokes/Darcy interface problem, where, Navier–Stokes- and Stokes/Darcy interface problems are reformulated to several elliptic interface problems in regard to pressure and velocity variables, respectively. Simultaneously, some augmented variables are introduced along the interface to regain the original interface conditions. Thus, the standard immersed interface method that is originally designed for the elliptic interface problem [20] now can be applied to Stokes-involved interface problems with a comparable approximation accuracy.

In this paper, we also intend to utilize the standard IFE P_1 space that is originally designed for the elliptic interface problem [23, 21] to solve more complicated interface problems involving multiple primary variables and/or different equations on either side of the interface, e.g., the Stokes interface problem (1)-(8) and the Stokes/elliptic interface problem (10)-(16), or more generally, FSI problems. Our idea is simpler than that of [24, 22], we keep the originally involved Stokes equations unchanged, and make the velocity $\boldsymbol{u}$ look like a "unique" primary variable by moving the pressure p to the right hand side of the jump flux interface condition (6) or (14), where, the pressure p is treated as a "known" variable that is updated in an

iterative process by solving the Stokes-involved interface problem for the pressure as well as the velocity via a specifically designed discretization method. Hence, the jump flux interface condition is iteratively updated as well along with the obtained pressure p by holding the same form as that of the elliptic interface problem in each iteration. Thus, the standard IFE P_1 space can be applied to the Stokes-involved interface problem by an iterative approach without introducing any artificial variables, if the aforementioned specific discretization method can be developed to solve interface problems with multiple primary variables on the body-unfitted mesh.

To that end, we employ a body-unfitted mesh method which is popularly adopted for solving FSI problems, the so-called distributed Lagrange multiplier/fictitious domain (DLM/FD) method [13, 14, 37, 36, 30, 7, 3, 6, 35], and appropriately integrate the IFE space into the DLM/FD finite element method, then finally develop a combined distributed Lagrange multiplier/fictitious domain–immersed finite element (DLM/FD-IFE) method, by which and the aforementioned iterative approach, the IFE space can thus be employed in a unified framework for the first time to solve FSI and other general interface problems that may bear different governing equations on either side of the interface.

The rest of this paper is organized as follows. In Section 2 we describe the iterative construction approach of immersed finite element spaces, as examples, for Stokes- and Stokes/elliptic interface problems since different interface conditions are involved. In Section 3, we shown how the newly defined iteratively constructed IFE spaces are integrated into the DLM/FD finite element method for Stokes- and Stokes/elliptic interface problems. Numerical experiments are carried out in Section 4 for both interface problems to illustrate an anticipated approximation accuracy and the efficiency of the proposed iterative approach.

2. An iterative approach for constructing IFE spaces

As an example, in this section we demonstrate how an iterative approach is developed for the purpose of constructing IFE spaces to deal with different interface conditions existing in Stokes interface problem (1)-(8) and Stokes/elliptic problem (10)-(16), respectively. Similar ideas can be extended to more general interface problems such as FSI.

2.1. The IFE space for interface conditions of Stokes interface problem.

We address in Section 1 that it is difficult to construct the immersed finite element space for Stokes interface problem that satisfies the interface conditions (5) and (6) since both unknowns, velocity $\boldsymbol{u}$ and pressure p, are involved in the jump flux condition (6). Such immersed finite element shape functions for both $\boldsymbol{u}$ and p are highly nontrivial and sometimes impossible without introducing extra interface conditions. Recently, an IFE Q_1/Q_0 space is defined in [2] for Stokes interface problem in an extremely sophisticated fashion and with extra interface conditions, in which a 16×16 linear system needs to be solved in each interface element to determine IFE Q_1/Q_0 shape functions. And, such IFE Q_1/Q_0 element is not even a stable Stokes-pair yet and the discontinuous Galerkin technique has to be applied together in order to stabilize the computation for Stokes interface problem.

To simplify the definition of IFE space for interface conditions (5) and (6), we attempt to employ the existing IFE space that is originally designed for the elliptic interface problem to discretize the velocity $\boldsymbol{u}$ only, at the same time, assuming that the pressure p is known and does not need to be discretized in the IFE space but still needs to be discretized in the standard finite element space. Numerically, the pressure p is computed by an iterative scheme under a prescribed initial value.

Thus, the pressure p existing in the jump flux interface condition (6) can be moved to the right hand side of (6) as known, and only the velocity $\boldsymbol{u}$ is remained on the left hand side of (6) playing as the "unique" primary variable. A regular IFE P_1 space for $\boldsymbol{u}$ is thus able to be constructed as we do for the elliptic interface problem [23, 21]. In the following, provided that the value of pressure p is given, we describe how an IFE space is defined for the velocity $\boldsymbol{u}$ of Stokes interface problem in a triangular interface element, as shown in Figure 2.

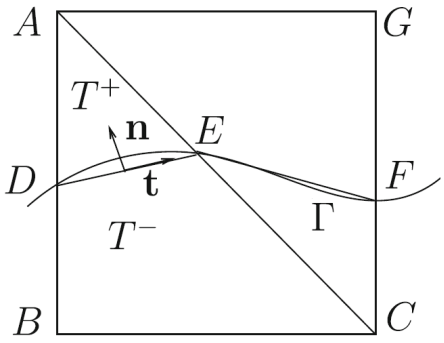

FIGURE 2. A typical interface element and a neighbouring element [18].

Let $T_h(\Omega)$ be a partition of Ω, independent of the location of the interface Γ, and $T_H(\Omega_2)$ be a partition of Ω_2. Further, let $T_h^{int} \subset T_h(\Omega)$ be the collection of interface elements which are cut through by the interface Γ. Associated with $T_h(\Omega)$ and $T_H(\Omega_2)$, we define continuous piecewise linear finite element spaces Q_h and $\boldsymbol{V}_{2,H}$, which are the subset of $Q = L^2(\Omega)$ and $\boldsymbol{V}_2 = (H^1(\Omega_2))^d$, respectively.

For a given pressure function $p \in Q_h$, we determine a piecewise linear function $\boldsymbol{\phi}(\boldsymbol{x}) = (\phi_1(\boldsymbol{x}), \phi_2(\boldsymbol{x}))^T$, $\boldsymbol{x} = (x_1, x_2)$, in a triangular interface element $T \in T_h^{int}$ by letting

$$\phi_i(x) = \begin{cases} \phi_i^+ = a_i^+ + b_i^+ x_1 + c_i^+ x_2, & \forall \boldsymbol{x} \in T^+, \\ \phi_i^- = a_i^- + b_i^- x_1 + c_i^- x_2, & \forall \boldsymbol{x} \in T^-, \end{cases} \tag{18}$$

where, we assume $T^+ \subset \Omega_1$, $T^- \subset \Omega_2$. For each $i = 1, 2$, six coefficients $a_i^{\pm}$, $b_i^{\pm}$, $c_i^{\pm}$ in (18) are chosen to satisfy the following six conditions

$$\phi_i(A) = u_i(A),\ \phi_i(B) = u_i(B),\ \phi_i(C) = u_i(C), \tag{19}$$

$$\phi_i^+(D) = \phi_i^-(D),\ \phi_i^+(E) = \phi_i^-(E), \tag{20}$$

$$\beta_1 \frac{\partial \phi_i^+}{\partial \boldsymbol{n}} - \beta_2 \frac{\partial \phi_i^-}{\partial \boldsymbol{n}} = \left(p(A) - \frac{p(B) + p(C)}{2} \right) n_i - w_i, \tag{21}$$

where, $\boldsymbol{w} = (w_1, w_2)^T$ is the jump flux, $\boldsymbol{n} = (n_1, n_2)^T$ is the unit outward normal vector pointing to T^+ from T^-, and $u_i(A)$, $u_i(B)$, $u_i(C)$ $(i = 1, 2)$ are nodal values of velocity $\boldsymbol{u} = (u_1, u_2)$. (21) is obtained by moving p to the right hand side of (6), and, thanks to the definition of piecewise linear function $p \in Q_h$ based on three vertices A, B and C in the immersed element T, we choose $p(A)$ as the piecewise constant value of $p \in T^+$, and $\frac{p(B)+p(C)}{2}$ as the piecewise constant value of $p \in T^-$. Then, (21) eventually becomes the jump flux condition serving the velocity $\boldsymbol{u}$, only.

Thus, provided that a pressure function $p \in Q_h$ is known, an immersed finite element space $\boldsymbol{V}_h^p$ can be defined as the set of all piecewise linear functions that satisfy

$$\begin{cases} \boldsymbol{\phi}\big|_T \text{ is the standard piecewise linear function if } T \in T_h(\Omega)\backslash T_h^{int}, \\ \boldsymbol{\phi}\big|_T \text{ is the immersed piecewise linear function defined in (18) – (21) if } T \in T_h^{int}, \\ \boldsymbol{\phi} \text{ is continuous at all nodal points}, \\ \boldsymbol{\phi} = \boldsymbol{0} \text{ on } \partial\Omega. \end{cases}$$

For a velocity function $\boldsymbol{u}(\boldsymbol{x})$ defined in Ω, we define $I_h^p \boldsymbol{u} \in \boldsymbol{V}_h^p$ as the interpolation function such that $I_h^p \boldsymbol{u}(\boldsymbol{x}_i) = \boldsymbol{u}(\boldsymbol{x}_i)$ for all nodal points $\boldsymbol{x}_i \in T_h(\Omega)$.

Remark 2.1. *Thanks to the proved error estimate of interpolation function* [23] *that is defined in the IFE space for the elliptic interface problem, where the approximation property of the IFE space is analyzed, we anticipate that the approximation capability of the above* $\boldsymbol{V}_h^p$ *shall be better than the regular* P_1 *continuous finite element space if the pressure is sufficiently smooth in each subdomain.*

2.2. The IFE space for interface conditions of Stokes/elliptic interface problem. To the authors' best knowledge, the IFE space that satisfies interface conditions (13) and (14) has not been studied yet for the Stokes/elliptic interface problem in the literature. Now with the similar idea of constructing the IFE space for the Stokes interface problem, we are able to define an IFE space for velocity $\boldsymbol{u}$ which satisfies the interface conditions (13) and (14) when the pressure p is provided, iteratively. Note that the main difference between this type of interface conditions and the interface conditions of Stokes interface problem (5) and (6) is that the pressure only exists in Ω_1 but is undefined in Ω_2.

For a given pressure function $p \in Q_{1,h} = Q_h|_{\Omega_1}$, we still define a piecewise linear function $\boldsymbol{\phi}(\boldsymbol{x}) = (\phi_1(\boldsymbol{x}), \phi_1(\boldsymbol{x}))^T$ in the interface element $T \in T_h^{int}$ satisfying (18), as shown in Figure 2, and six coefficients are chosen such that

$$\phi_i(A) = u_i(A),\ \phi_i(B) = u_i(B),\ \phi_i(C) = u_i(C), \tag{22}$$

$$\phi_i^+(D) = \phi_i^-(D),\ \phi_i^+(E) = \phi_i^-(E), \tag{23}$$

$$\beta_1 \frac{\partial \phi_i^+}{\partial \boldsymbol{n}} - \beta_2 \frac{\partial \phi_i^-}{\partial \boldsymbol{n}} = \begin{cases} -w_i + p(A)n_i, & \text{if } A \in \Omega_1 \\ -w_i - \frac{p(B)+p(C)}{2} n_i, & \text{if } A \notin \Omega_1 \end{cases} \tag{24}$$

where, we assume the unit outward normal vector $\boldsymbol{n} = (n_1, n_2)^T$ points to $T^+ \subset \Omega_1$ from $T^- \subset \Omega_2$. (24) is obtained by moving p to the right hand side of (14), and, since the piecewise linear function $p \in Q_{1,h}$ is defined with its nodal values on three vertices A, B and C, we pick either $p(A)$ or $\frac{p(B)+p(C)}{2}$ as the piecewise constant value of $p \in \Omega_1$ by determining which vertex (or vertices) belong(s) to Ω_1. Then, (24) eventually becomes the jump flux condition serving the velocity $\boldsymbol{u}$, only.

Thus, provided that a pressure function p is known, an IFE space $\boldsymbol{W}_h^p$ can be defined as the set of all piecewise linear functions that satisfy

$$\begin{cases} \boldsymbol{\phi}\big|_T \text{ is the linear piecewise function if } T \in T_h(\Omega)\backslash T_h^{int}, \\ \boldsymbol{\phi}\big|_T \text{ is the immersed piecewise linear function defined in (22) – (24) if } T \in T_h^{int}, \\ \boldsymbol{\phi} \text{ is continuous at all nodal points}, \\ \boldsymbol{\phi} = \boldsymbol{0} \text{ on } \partial\Omega. \end{cases}$$

To end this section, we underline that an iterative approach for constructing the immersed finite element space needs to be developed for Stokes- and Stokes/elliptic interface problems, respectively, in order to complete the definition of the IFE spaces $\boldsymbol{V}_h^p$ and $\boldsymbol{W}_h^p$. In summary, the general idea of the iterative construction

approach is that, in each iteration, we only choose one primary variable to be remained on the left hand side of jump flux interface condition, and move other involved primary variables to the right hand side by taking the numerical results of those variables from the last iteration step as their values. Moreover, in order to obtain numerical results of those updated variables, we shall integrate such iteration process with a specifically developed finite element discretization method based upon the newly defined IFE space to solve the involved interface problem for all primary variables. Such specific finite element discretization method is crucial to be capable of solving the interface problem with different governing equations on either side of the interface, and will be discussed in the next section. We remark here that ideas of such new approach of constructing IFE spaces can be similarly applied to other kinds of interface conditions than examples shown in this section.

3. The combined distributed Lagrange multiplier/fictitious domain - immersed finite element method

In this section, we integrate the iteratively constructed IFE space with the DLM/FD method that has been long adopted but just recently analyzed for interface problems including FSI [36, 8, 4, 6, 35, 26, 33, 34], and present a unified approach, the combined distributed Lagrange multiplier/fictitious domain–immersed finite element (DLM/FD-IFE) method, that can deal with various interface problems with different interface conditions. In what follows, we utilize the Stokes- and Stokes/elliptic interface problem as examples to show how to apply the proposed method to general interface problems.

3.1. Application to Stokes interface problem. Introduce $\boldsymbol{V} = \left(H_0^1(\Omega)\right)^d$, $Q = L^2(\Omega)$ and $\boldsymbol{\Lambda} = [(H^1(\Omega_2))^d]^*$ that is the dual space of $\boldsymbol{V}_2 = (H^1(\Omega_2))^d$. Let $\langle\cdot,\cdot\rangle_{\Omega_2}$ denote the duality pairing between $\boldsymbol{\Lambda}$ and $\boldsymbol{V}_2$.

Then the standard weak form of (1)-(8) can be defined as follows. Find $(\boldsymbol{u}, p) \in \boldsymbol{V} \times Q$ with $\boldsymbol{u}|_{\Omega_1} = \boldsymbol{u}_1,\ \boldsymbol{u}|_{\Omega_2} = \boldsymbol{u}_2,\ p|_{\Omega_1} = p_1,\ p|_{\Omega_2} = p_2$ such that

$$(\beta\nabla\boldsymbol{u}, \nabla\boldsymbol{v})_\Omega - (p, \nabla\cdot\boldsymbol{v})_\Omega = (\boldsymbol{f}, \boldsymbol{v})_\Omega + (\boldsymbol{w}, \boldsymbol{v})_\Gamma, \quad \forall \boldsymbol{v} \in \boldsymbol{V}, \tag{25}$$

$$(\nabla\cdot\boldsymbol{u}, q)_\Omega = 0, \quad \forall q \in Q. \tag{26}$$

And, the weak form of the DLM/FD method for (1)-(8) can be defined as follows [26]. Find $(\tilde{\boldsymbol{u}},\ \boldsymbol{u}_2,\ \tilde{p},\ \boldsymbol{\lambda}) \in \boldsymbol{V} \times \boldsymbol{V}_2 \times Q \times \boldsymbol{\Lambda}$ such that

$$(\tilde{\beta}\nabla\tilde{\boldsymbol{u}}, \nabla\boldsymbol{v})_\Omega - (\tilde{p}, \nabla\cdot\boldsymbol{v})_\Omega + \langle\boldsymbol{\lambda}, \boldsymbol{v}|_{\Omega_2}\rangle_{\Omega_2} = (\tilde{\boldsymbol{f}}, \boldsymbol{v})_\Omega, \tag{27}$$

$$(\nabla\cdot\tilde{\boldsymbol{u}}, q)_\Omega = 0, \tag{28}$$

$$\begin{aligned}\left((\beta_2 - \tilde{\beta})\nabla\boldsymbol{u}_2, \nabla\boldsymbol{v}_2\right)_{\Omega_2} - \langle\boldsymbol{\lambda}, \boldsymbol{v}_2\rangle_{\Omega_2} \\ = \left(\boldsymbol{f}_2 - \tilde{\boldsymbol{f}}_2, \boldsymbol{v}_2\right)_{\Omega_2} + (\boldsymbol{w}, \boldsymbol{v}_2)_\Gamma,\end{aligned} \tag{29}$$

$$\langle\boldsymbol{\xi}, \tilde{\boldsymbol{u}}|_{\Omega_2} - \boldsymbol{u}_2\rangle_{\Omega_2} = 0, \tag{30}$$

$$\forall(\boldsymbol{v},\ \boldsymbol{v}_2,\ q,\ \boldsymbol{\xi}) \in \boldsymbol{V} \times \boldsymbol{V}_2 \times Q \times \boldsymbol{\Lambda},$$

where, $\tilde{\beta}$ is a smooth extension of β_1 to Ω_2 thus is defined in the entire domain Ω, i.e., $\tilde{\beta}|_{\Omega_1} = \beta_1, \tilde{\beta}|_{\Omega_2} = \tilde{\beta}_2$. Corresponding to the extension function $\tilde{\beta}$, $\tilde{\boldsymbol{f}}_2$ is also a smooth extension of $\boldsymbol{f}_1$ to Ω_2, denoted by $\tilde{\boldsymbol{f}}$ such that $\tilde{\boldsymbol{f}}|_{\Omega_1} = \boldsymbol{f}_1,\ \tilde{\boldsymbol{f}}|_{\Omega_2} = \tilde{\boldsymbol{f}}_2$. Then $\tilde{\boldsymbol{f}} \in (L^2(\Omega))^d$, $\tilde{\beta} \in L^\infty(\Omega)$. In general, $\tilde{\beta}_2 \neq \beta_2,\ \tilde{\boldsymbol{f}}_2 \neq \boldsymbol{f}_2$. As a consequence, the solution $(\tilde{\boldsymbol{u}}, \tilde{p}) \in \boldsymbol{V} \times Q$ satisfy $\tilde{\boldsymbol{u}}|_{\Omega_1} = \boldsymbol{u}_1,\ \tilde{\boldsymbol{u}}|_{\Omega_2} = \tilde{\boldsymbol{u}}_2,\ \tilde{p}|_{\Omega_1} = p_1,\ \tilde{p}|_{\Omega_2} = \tilde{p}_2$, and $\tilde{\boldsymbol{u}}|_{\partial\Omega} = 0$, and $\tilde{\boldsymbol{u}}|_\Gamma = \boldsymbol{u}_1|_\Gamma = \boldsymbol{u}_2|_\Gamma$. Due to the equivalence between the

DLM/FD weak form (27)-(30) and the standard weak form (25)-(26) [26], the following regularity results hold for the solution $(\tilde{\boldsymbol{u}}, \tilde{p})$ as well

$$\tilde{\boldsymbol{u}} \in \boldsymbol{X}, \quad \tilde{p} \in \boldsymbol{Y}. \tag{31}$$

In addition, we require the following condition in order to obtain the well-posedness of the DLM/FD method (27)-(30) [26]

$$\infty > \bar{\beta} \geq \beta_2 > \tilde{\beta} \geq \underline{\beta} > 0, \quad \beta_2 - \tilde{\beta} \geq \underline{\beta} > 0, \tag{32}$$

where, $\underline{\beta}$ and $\bar{\beta}$ are positive constants.

As shown in [8, 26], we can associate to any $\boldsymbol{\xi} \in \boldsymbol{\Lambda}$ an element of $\boldsymbol{\psi} \in \boldsymbol{V}_2$ which is the solution of the following variational equation

$$(\boldsymbol{\psi}, \boldsymbol{v})_{\boldsymbol{V}_2} = \langle \boldsymbol{\xi}, \boldsymbol{v} \rangle_{\Omega_2}, \quad \forall \boldsymbol{v} \in \boldsymbol{V}_2, \tag{33}$$

where $(\cdot,\cdot)_{\boldsymbol{V}_2}$ represents the H^1-inner product in $\boldsymbol{V}_2$, defined as

$$(\boldsymbol{\psi}, \boldsymbol{v})_{\boldsymbol{V}_2} = (\boldsymbol{\psi}, \boldsymbol{v})_{\Omega_2} + (\nabla \boldsymbol{\psi}, \nabla \boldsymbol{v})_{\Omega_2}. \tag{34}$$

It is easy to show that there exists a unique $\boldsymbol{\psi} \in \boldsymbol{V}_2$ satisfying (33). In addition, the following equality can be easily obtained [8]

$$\|\boldsymbol{\xi}\|_{\boldsymbol{\Lambda}} = \|\boldsymbol{\psi}\|_{\boldsymbol{V}_2}. \tag{35}$$

Thus, (30) is equivalent with the following equation by letting $\boldsymbol{v} = \tilde{\boldsymbol{u}}|_{\Omega_2} - \boldsymbol{u}_2$ in (33)

$$(\boldsymbol{\psi}, \tilde{\boldsymbol{u}}|_{\Omega_2} - \boldsymbol{u}_2)_{\boldsymbol{V}_2} = 0, \quad \forall \boldsymbol{\psi} \in \boldsymbol{V}_2. \tag{36}$$

The well-posedness of the above DLM/FD weak form (27)-(30), which is actually a nested saddle-point problem induced by both Stokes equations and DLM/FD method in regard to Stokes variables (velocity and pressure) and Lagrange multipliers, are proved in [26] by verifying that the *inf-sup* condition is held for a sophisticated bilinear form of (27)-(30) and using the Babuška–Brezzi's theory [5, 9].

According to the equivalence of (30) and (36), and employing the newly defined IFE space $\boldsymbol{V}_h^{p_h}$ to discretize the velocity $\boldsymbol{u}_h$ that is defined in the entire domain Ω, provided that the pressure p_h is iteratively given, we can define the DLM/FD-IFE method for (27)-(30) as follows. Find $(\boldsymbol{u}_h,\ \boldsymbol{u}_{2,H},\ p_h,\ \boldsymbol{\phi}_H) \in \boldsymbol{V}_h^{p_h} \times \boldsymbol{V}_{2,H} \times Q_h \times \boldsymbol{V}_{2,H}$ such that

$$\left(\tilde{\beta}\nabla \boldsymbol{u}_h, \nabla \boldsymbol{v}_h\right)_{\Omega} - (p_h, \nabla \cdot \boldsymbol{v}_h)_{\Omega} + d_h(p_h, p_h) + \langle \boldsymbol{\phi}_H, \boldsymbol{v}_h|_{\Omega_2} \rangle_{\boldsymbol{V}_2} = \left(\tilde{\boldsymbol{f}}, \boldsymbol{v}_h\right)_{\Omega}, \tag{37}$$

$$(\nabla \cdot \boldsymbol{u}_h, q_h)_{\Omega} = 0, \tag{38}$$

$$\left((\beta_2 - \tilde{\beta})\nabla \boldsymbol{u}_{2,H}, \nabla \boldsymbol{v}_{2,H}\right)_{\Omega_2} - \langle \boldsymbol{\phi}_H, \boldsymbol{v}_{2,H} \rangle_{\boldsymbol{V}_2} = \left(\boldsymbol{f}_2 - \tilde{\boldsymbol{f}}_2, \boldsymbol{v}_{2,H}\right)_{\Omega_2} + (\boldsymbol{w}, \boldsymbol{v}_{2,H})_{\Gamma}, \tag{39}$$

$$\langle \boldsymbol{\psi}_H, \boldsymbol{u}_h|_{\Omega_2} - \boldsymbol{u}_{2,H} \rangle_{\boldsymbol{V}_2} = 0, \tag{40}$$

$$\forall (\boldsymbol{v}_h,\ \boldsymbol{v}_{2,H},\ q_h,\ \boldsymbol{\psi}_H) \in \boldsymbol{V}_h^{p_h} \times \boldsymbol{V}_{2,H} \times Q_h \times \boldsymbol{V}_{2,H},$$

where, since the unstable P_1-P_1 mixed element is used in the above scheme for the convenience of constructing the standard IFE P_1 space for the velocity $\boldsymbol{u}_h$ [21, 23], we introduce the following Galerkin/Least-squares (GLS)-type pressure-stabilization term [25] in (37) to stabilize the above saddle-point problem that is transformed from the original interface problem by the DLM/FD method

$$d_h(p, q) = C_\delta \frac{h^2}{\|\tilde{\beta}\|_{\infty,\Omega}} (\nabla p, \nabla q)_{\Omega}, \tag{41}$$

where, C_δ is a constant that needs to be tuned in the computation.

Following an analogous mixed finite element error analysis demonstrated in [26], we can have the following a priori error estimate hold for (37)-(40)

$$\begin{aligned}&\|\tilde{\boldsymbol{u}}-\boldsymbol{u}_h\|_{\boldsymbol{V}}+\|\boldsymbol{u}_2-\boldsymbol{u}_{2,H}\|_{\boldsymbol{V}_2}+\|\tilde{p}-p_h\|_Q+\|\boldsymbol{\phi}-\boldsymbol{\phi}_H\|_{\boldsymbol{V}_2}\\ \leq & C\left(\inf_{\boldsymbol{v}_h\in\boldsymbol{V}_h^{p_h}}\|\tilde{\boldsymbol{u}}-\boldsymbol{v}_h\|_{\boldsymbol{V}}+\inf_{\boldsymbol{v}_{2,H}\in\boldsymbol{V}_{2,H}}\|\boldsymbol{u}_2-\boldsymbol{v}_{2,H}\|_{\boldsymbol{V}_2}+\inf_{q_h\in Q_h}\|\tilde{p}-q_h\|_Q\right.\\ &\left.+H(\|\tilde{p}\|_{H^1(\Omega_2)}+\|\boldsymbol{u}_2\|_{\boldsymbol{V}_2}+\|(\tilde{\beta}/\beta_2)\boldsymbol{f}_2-\tilde{\boldsymbol{f}}\|_{(L^2(\Omega_2))^d})\right),\end{aligned}\tag{42}$$

where, the finite element space of velocity, $\boldsymbol{V}_h$, is replaced by the iteratively constructed IFE space $\boldsymbol{V}_h^{p_h}$.

To obtain the approximation solution of the above DLM/FD-IFE method, we need to iteratively solve (37)-(40) with a prescribed initial value of pressure, $p_h^{(0)}$. The following iterative process is employed.

Algorithm 3.1. *First, an initial value for the pressure, $p_h^{(0)}$, is appropriately chosen. Then for $m=1,2,\cdots$, the following steps are conducted in each step:*

(1) Define the IFE space $\boldsymbol{V}_h^{p_h^{(m-1)}}$;

(2) Solve (37)-(40) for $\left(\boldsymbol{u}_h^{(m)},\ \boldsymbol{u}_{2,H}^{(m)},\ p_h^{(m)}\right)\in\boldsymbol{V}_h^{p_h^{(m-1)}}\times\boldsymbol{V}_{2,H}\times Q_h$;

(3) When $m\geq 2$, determine if the following iterative errors reach the given tolerance ε:

$$\|\boldsymbol{u}_h^{(m)}-\boldsymbol{u}_h^{(m-1)}\|_{0,\Omega}+\|\boldsymbol{u}_{2,H}^{(m)}-\boldsymbol{u}_{2,H}^{(m-1)}\|_{0,\Omega_2}+\|p_h^{(m)}-p_h^{(m-1)}\|_{0,\Omega}\leq\varepsilon.$$

If yes, then stop the iteration; otherwise, let $m\Leftarrow m+1$, go to Step (1).

Remark 3.2. *Instead of P_1 continuous finite element space, we employ the iteratively constructed IFE space $\boldsymbol{V}_h^{p_h}$ for the approximation of velocity $\tilde{\boldsymbol{u}}$ in (37)-(40), which is reflected in the first term of the right hand side of (42), i.e., the interpolation error estimate of the velocity $\tilde{\boldsymbol{u}}$. Due to the regularity results (31) showing that $\tilde{\boldsymbol{u}}\in H^s(\Omega)$ $(1<s<1.5)$, the a priori interpolation error of $\tilde{\boldsymbol{u}}$ in the standard finite element P_1 space $\boldsymbol{V}_h$ supposes to be $\inf_{\boldsymbol{v}_h\in\boldsymbol{V}_h}\|\tilde{\boldsymbol{u}}-\boldsymbol{v}_h\|_{\boldsymbol{V}}\leq Ch^{s-1}\|\tilde{\boldsymbol{u}}\|_{H^s(\Omega)}$, i.e., one half order convergence rate at most if using the standard finite element P_1 space $\boldsymbol{V}_h$. Now with the iteratively constructed IFE space $\boldsymbol{V}_h^{p_h}$, we anticipate an improved convergence order for $\inf_{\boldsymbol{v}_h\in\boldsymbol{V}_h^{p_h}}\|\tilde{\boldsymbol{u}}-\boldsymbol{v}_h\|_{\boldsymbol{V}}$ up to optimal: the first order in H^1 norm. According to (42), this further delivers the optimal error estimates for discretization errors of the velocity, $\|\tilde{\boldsymbol{u}}-\boldsymbol{u}_h\|_{\boldsymbol{V}}$, with the first order, and of the pressure, $\|\tilde{p}-p_h\|_Q$, with the second order, as validated in Section 4.1. A (nearly) optimal error estimate in L^2 norm (the second order convergence rate) for velocity is also illustrated in Section 4, which is correct due to the Aubin–Nitsche duality argument as a standard finite element theory.*

Remark 3.3. *In practice, because P_1-P_1 element is used to discretize the nested saddle-point system derived by the above DLM/FD-IFE method, the approximation accuracy of pressure p_h is affected by the performance of the stabilization term $d_h(p,q)$ shown in (41) that is influenced by the choice of the stabilization parameter C_δ, i.e., the optimal convergence of pressure depends on an appropriately chosen C_δ.*

Remark 3.4. *Such iteratively constructed immersed finite element space can be integrated into other discretization schemes. For example, based on the weak form*

(25)-(26), *we can directly develop an immersed finite element method for Stokes interface problem* (1)-(8) *without combining with the DLM/FD method, which is, however, impossible for the Stokes/elliptic interface problem as shown in the next section.*

Remark 3.5. *The iterative process shown in Algorithm 3.1 is expected to be convergent within a few steps if the jump of pressure across the interface* Γ *in the immersed elements is relatively small, resulting in a nearly unchanged condition (21) after several iterations. A good initial value* p_h^0 *is also important to accelerate the convergence of the iteration.*

3.2. Application to Stokes/elliptic problem. In this section, we develop the DLM/FD-IFE method for a type of linearized steady state FSI problem that is essentially the Stokes/elliptic interface problem as defined in (10)-(16).

The standard weak form of (10)-(16) can be defined as follows. Find $(\boldsymbol{u}, p) \in \boldsymbol{V} \times L^2(\Omega_1)$ with $\boldsymbol{u}|_{\Omega_1} = \boldsymbol{u}_1,\ \boldsymbol{u}|_{\Omega_2} = \boldsymbol{u}_2,\ p|_{\Omega_1} = p_1$, such that

$$(\beta \nabla \boldsymbol{u}, \nabla \boldsymbol{v})_\Omega - (p, \nabla \cdot \boldsymbol{v})_{\Omega_1} = (\boldsymbol{f}, \boldsymbol{v})_\Omega + (\boldsymbol{w}, \boldsymbol{v})_\Gamma, \quad \forall \boldsymbol{v} \in \boldsymbol{V}, \tag{43}$$

$$(\nabla \cdot \boldsymbol{u}, q)_{\Omega_1} = 0, \quad \forall q \in L^2(\Omega_1). \tag{44}$$

One weak form of the DLM/FD method for (10)-(16) is to find $(\tilde{\boldsymbol{u}},\ \boldsymbol{u}_2,\ \tilde{p},\ \boldsymbol{\lambda}) \in \boldsymbol{V} \times \boldsymbol{V}_2 \times Q \times \boldsymbol{\Lambda}$ such that [33]

$$(\tilde{\beta} \nabla \tilde{\boldsymbol{u}}, \nabla \boldsymbol{v})_\Omega - (\tilde{p}, \nabla \cdot \boldsymbol{v})_\Omega + \langle \boldsymbol{\lambda}, \boldsymbol{v}|_{\Omega_2} \rangle_{\Omega_2} = (\tilde{\boldsymbol{f}}, \boldsymbol{v})_\Omega, \tag{45}$$

$$(\nabla \cdot \tilde{\boldsymbol{u}}, q)_\Omega - (\nabla \cdot \tilde{\boldsymbol{u}}_2, q)_{\Omega_2} = 0, \tag{46}$$

(47)

$$\Big((\beta_2 - \tilde{\beta}) \nabla \boldsymbol{u}_2, \nabla \boldsymbol{v}_2\Big)_{\Omega_2} + (p|_{\Omega_2}, \nabla \cdot, \boldsymbol{v}_2)_{\Omega_2} - \langle \boldsymbol{\lambda}, \boldsymbol{v}_2 \rangle_{\Omega_2} = \Big(\boldsymbol{f}_2 - \tilde{\boldsymbol{f}}|_{\Omega_2}, \boldsymbol{v}_2\Big)_{\Omega_2} + (\boldsymbol{w}, \boldsymbol{v}_2)_\Gamma,$$

$$\langle \boldsymbol{\xi}, \tilde{\boldsymbol{u}}|_{\Omega_2} - \boldsymbol{u}_2 \rangle_{\Omega_2} = 0, \tag{48}$$

$$\forall (\boldsymbol{v},\ \boldsymbol{v}_2,\ q,\ \boldsymbol{\xi}) \in \boldsymbol{V} \times \boldsymbol{V}_2 \times Q \times \boldsymbol{\Lambda},$$

where, we do the same smooth extension for β_1 and $\boldsymbol{f}_1$ to obtain $\tilde{\beta} \in L^\infty(\Omega)$ and $\tilde{\boldsymbol{f}} \in (L^2(\Omega))^d$, respectively. And, the solution $(\tilde{\boldsymbol{u}}, \tilde{p}) \in \boldsymbol{V} \times Q$ satisfy $\tilde{\boldsymbol{u}}|_{\Omega_1} = \boldsymbol{u}_1,\ \tilde{\boldsymbol{u}}|_{\Omega_2} = \tilde{\boldsymbol{u}}_2,\ \tilde{p}|_{\Omega_1} = p_1,\ \tilde{p}|_{\Omega_2} = \tilde{p}_2$, and $\tilde{\boldsymbol{u}}|_{\partial\Omega} = 0$, and $\tilde{\boldsymbol{u}}|_\Gamma = \boldsymbol{u}_1|_\Gamma = \boldsymbol{u}_2|_\Gamma$. The equivalence between the DLM/FD weak form (45)-(48) and the standard weak form (43)-(44) [33] results that $(\tilde{\boldsymbol{u}}, \tilde{p})$ hold the same regularity results as shown in (31). For the same reason as shown in Section 3.1, (48) is equivalent with (36).

Note that the DLM/FD method for Stoke/elliptic interface problem (45)-(48) also forms a nested saddle-point problem that includes two subproblems of saddle-point type: the inside one from Stokes equations, and the outside one from the DLM/FD method itself regarding Lagrange multiplier and Stokes unknowns (velocity and pressure). Please refer to [33] for the well-posedness of (45)-(48), where, a monolithic bilinear form is proved to hold the *inf-sup* condition upon the Babuška–Brezzi's theory [5, 9].

Similarly, the combined DLM/FD-IFE method for Stokes/elliptic interface problem (10)-(16) can be defined as follows [33]. Find $(\boldsymbol{u}_h,\ \boldsymbol{u}_{2,H},\ p_h,\ \boldsymbol{\phi}_H) \in \boldsymbol{W}_h^{p_h} \times$

$\boldsymbol{V}_{2,H} \times Q_h \times \boldsymbol{V}_{2,H}$ such that

$$\left(\tilde{\beta}\nabla \boldsymbol{u}_h, \nabla \boldsymbol{v}_h\right)_\Omega - (p_h, \nabla\cdot \boldsymbol{v}_h)_\Omega + d_h(p_h, p_h) + (\boldsymbol{\phi}_H, \boldsymbol{v}_h|_{\Omega_2})_{\boldsymbol{V}_2} = \left(\tilde{\boldsymbol{f}}, \boldsymbol{v}_h\right)_\Omega, \tag{49}$$

$$(\nabla\cdot \boldsymbol{u}_h, q_h)_\Omega - (\nabla\cdot \boldsymbol{u}_{2,H}, q_h)_{\Omega_2} = 0, \tag{50}$$

$$\begin{aligned}\left((\beta_2-\tilde{\beta})\nabla \boldsymbol{u}_{2,H}, \nabla \boldsymbol{v}_{2,H}\right)_{\Omega_2} + (p_h|_{\Omega_2}, \nabla\cdot \boldsymbol{v}_{2,H})_{\Omega_2} - (\boldsymbol{\phi}_H, \boldsymbol{v}_{2,H})_{\boldsymbol{V}_2}\\ = \left(\boldsymbol{f}_2 - \tilde{\boldsymbol{f}}|_{\Omega_2}, \boldsymbol{v}_{2,H}\right)_{\Omega_2} + (\boldsymbol{w}, \boldsymbol{v}_{2,H})_\Gamma,\end{aligned} \tag{51}$$

$$(\boldsymbol{\psi}_H, \boldsymbol{u}_h|_{\Omega_2} - \boldsymbol{u}_{2,H})_{\boldsymbol{V}_2} = 0, \tag{52}$$

$$\forall\, (\boldsymbol{v}_h,\ \boldsymbol{v}_{2,H},\ q_h,\ \boldsymbol{\psi}_H) \in \boldsymbol{W}_h^{p_h} \times \boldsymbol{V}_{2,H} \times Q_h \times \boldsymbol{V}_{2,H},$$

where, the pressure-stabilization term, $d_h(p,q)$, is still needed to stabilize the P_1-P_1 element for the above saddle-point system.

An analogous mixed finite element error analysis [33] can be carried out for (49)-(52), and the following a priori error estimate can be derived based on the developed IFE space $\boldsymbol{W}_h^{p_h}$.

$$\begin{aligned}&\|\tilde{\boldsymbol{u}} - \boldsymbol{u}_h\|_{\boldsymbol{V}} + \|\boldsymbol{u}_2 - \boldsymbol{u}_{2,H}\|_{\boldsymbol{V}_2} + \|\tilde{p} - p_h\|_Q + \|\boldsymbol{\phi} - \boldsymbol{\phi}_H\|_{\boldsymbol{V}_2}\\ &\le C\Big(\inf_{\boldsymbol{v}_h\in \boldsymbol{W}_h^{p_h}} \|\tilde{\boldsymbol{u}} - \boldsymbol{v}_h\|_{\boldsymbol{V}} + \inf_{\boldsymbol{v}_{2,H}\in \boldsymbol{V}_{2,H}} \|\boldsymbol{u}_2 - \boldsymbol{v}_{2,H}\|_{\boldsymbol{V}_2} + \inf_{q_h\in Q_h} \|\tilde{p} - q_h\|_Q\\ &\quad + H(\|\tilde{p}\|_{H^1(\Omega_2)} + \|\tilde{\boldsymbol{u}}\|_{(H^r(\Omega_1\cup\Omega_2))^d} + \|(\tilde{\beta}/\beta_2)\boldsymbol{f}_2 - \tilde{\boldsymbol{f}}\|_{(L^2(\Omega_2))^d})\Big),\end{aligned} \tag{53}$$

where, the finite element space of velocity, $\boldsymbol{V}_h$, is replaced by the iteratively constructed IFE space $\boldsymbol{W}_h^{p_h}$.

To apply the newly defined immersed finite element space, $\boldsymbol{W}_h^{p_h}$, to the above DLM/FD-IFE method (49)-(52) with an iteratively obtained pressure p_h, an iterative process that is similar with Algorithm 3.1 is needed to solve (49)-(52), as shown below.

Algorithm 3.6. *First, an initial value for the pressure, $p_h^{(0)}$, is appropriately chosen. Then, for $m = 1, 2, \cdots$, the following steps are iterated until convergence: First, an initial value for the pressure, $p_h^{(0)}$, is appropriately chosen. Then for $m = 1, 2, \cdots$, the following steps are conducted in each step:*

(1) Define the IFE space $\boldsymbol{W}_h^{p_h^{(m-1)}}$;

(2) Solve (49)-(52) for $\left(\boldsymbol{u}_h^{(m)},\ \boldsymbol{u}_{2,H}^{(m)},\ p_h^{(m)}\right) \in \boldsymbol{W}_h^{p_h^{(m-1)}} \times \boldsymbol{V}_{2,H} \times Q_h$;

(3) When $m \ge 2$, determine if the following iterative errors reach the given tolerance ε:

$$\|\boldsymbol{u}_h^{(m)} - \boldsymbol{u}_h^{(m-1)}\|_{0,\Omega} + \|\boldsymbol{u}_{2,H}^{(m)} - \boldsymbol{u}_{2,H}^{(m-1)}\|_{0,\Omega_2} + \|p_h^{(m)} - p_h^{(m-1)}\|_{0,\Omega} \le \varepsilon.$$

If yes, then stop the iteration; otherwise, let $m \Leftarrow m+1$, go to Step (1).

Remark 3.7. *For the Stokes/elliptic problem, the pressure, p, is only defined in Ω_1. However, in the DLM/FD-IFE method (49)-(52), the approximation to the pressure, i.e., p_h, is defined in the global domain Ω due to the introduction of the distributed Lagrange multiplier. This makes it possible for us to construct the IFE space for the velocity by the iterative approach.*

Remark 3.8. *Similar with the DLM/FD-IFE method for the Stokes interface problem (37)-(40), due to the iteratively constructed IFE space $\boldsymbol{W}_h^{p_h}$, we may gain the first order convergence for $\|\tilde{\boldsymbol{u}} - \boldsymbol{u}_h\|_{\boldsymbol{V}}$ and the second order convergence for $\|\tilde{p} - p_h\|_Q$, if the P_1-P_1 mixed element with pressure stabilizations works optimally for solving (49)-(52).*

4. Numerical experiments

In this section, we conduct some numerical experiments to validate the performance of the developed DLM/FD-IFE method for Stokes- and Stokes/elliptic interface problems with jump conditions across the interface.

Note that (21) and (24) are inhomogeneous jump conditions, in order to enforce them in each nodal basis function of the velocity in finite elements, we need to employ the velocity value, $\boldsymbol{u}_h^{(m)} = \left(u_{h,1}^{(m)}, u_{h,2}^{(m)}\right)^T$ obtained in the last iteration (the m-th step), as illustrated below. For example, considering the Stokes interface problems, we define the nodal basis function ϕ_B for $u_{h,1}^{(m)}$ and ψ_B for $u_{h,2}^{(m)}$ associated with the node B of the triangular interface element T shown in Fig. 2 by letting ϕ_B satisfy

$$\phi_B(A) = 0,\ \phi_B(B) = 1,\ \phi_B(C) = 0, \tag{54}$$

$$\phi_B^+(D) = \phi_B^-(D),\ \phi_B^+(E) = \phi_B^-(E), \tag{55}$$

$$\left(\beta_1 \frac{\partial \phi_B^+}{\partial \boldsymbol{n}} - \beta_2 \frac{\partial \phi_B^-}{\partial \boldsymbol{n}}\right) = S_{B,1}\left(\left(p(A) - \frac{p(B)+p(C)}{2}\right) n_1 - w_1\right), \tag{56}$$

and letting ψ_B satisfy

$$\psi_B(A) = 0,\ \psi_B(B) = 1,\ \psi_B(C) = 0, \tag{57}$$

$$\psi_B^+(D) = \psi_B^-(D),\ \psi_B^+(E) = \psi_B^-(E), \tag{58}$$

$$\left(\beta_1 \frac{\partial \psi_B^+}{\partial \boldsymbol{n}} - \beta_2 \frac{\partial \psi_B^-}{\partial \boldsymbol{n}}\right) = S_{B,2}\left(\left(p(A) - \frac{p(B)+p(C)}{2}\right) n_2 - w_2\right), \tag{59}$$

where,

$$S_{B,i} = \frac{\operatorname{sign}\left(u_{h,i}^{(m)}(B)\right)}{\left|u_{h,i}^{(m)}(A)\right| + \left|u_{h,i}^{(m)}(B)\right| + \left|u_{h,i}^{(m)}(C)\right|}. \tag{60}$$

The above definitions of nodal basis functions can be similarly applied to other element nodes A and C by following $\phi_i(j) = \delta_{ij}$ in (54) and $\psi_i(j) = \delta_{ij}$ in (57) for $i, j = A, B, C$, as well as to Stokes-elliptic problems.

It is easy to see that if

$$\left|u_{h,i}^{(m)}(A)\right| + \left|u_{h,i}^{(m)}(B)\right| + \left|u_{h,i}^{(m)}(C)\right| \neq 0, \tag{61}$$

then

$$S_{A,i} u_{h,i}^{(m)}(A) + S_{B,i} u_{h,i}^{(m)}(B) + S_{C,i} u_{h,i}^{(m)}(C) = 1, \quad (i = 1, 2). \tag{62}$$

(62) implies that the numerical solution $\boldsymbol{u}_h^{(m)}$ in each interface element T, which is the linear combination of its nodal basis functions at each node of element T defined in (54)-(59), satisfies the conditions (19)-(21) and (22)-(24), further the flux jump condition (6), except for the case that the values of $\boldsymbol{u}_h^{(m)}$ at each node of the interface element T are all zero. In such an extreme case, instead of using the IFE nodal basis functions as defined above, we may adopt the standard continuous piecewise linear finite element basis functions in this interface element T to avoid the zero denominator in (60), thus the jump condition (21) and (24) may not exactly hold for this extreme case. However, we want to point out that such extreme case does not happen either in our numerical experiments or in the realistic FSI problem, where the velocity values in the interface elements along with a moving interface are always nonzero. On the other hand, we also plan to study a remedy for this

extreme case in our next paper even it rarely happens, where, an immersed finite element space will be introduce for the pressure as well in the discretization scheme in order to construct nodal basis functions of velocity to satisfy the jump condition (21) and (24) even though the nodal values of velocity at all vertices are zero.

In the sequence, we consider the domain $\Omega = (0,1)^2$ cut by the circular interface $(x-0.3)^2+(y-0.3)^2 = 0.01$ that separates Ω into two regions $\Omega_1 = \{(x,y)^T : (x-0.3)^2 + (y-0.3)^2 > 0.01\}$ and $\Omega_2 = \{(x,y)^T : (x-0.3)^2 + (y-0.3)^2 < 0.01\}$, in which we define the following two examples of interface problems.

4.1. Example 1: Stokes interface problems. The following functions $\boldsymbol{u} = (u_1, u_2)^T$ and p are chosen as the real solutions of (1)-(8) by properly defining the right hand side functions $\boldsymbol{f}_1$, $\boldsymbol{f}_2$ and the jump flux function $\boldsymbol{w}$:

$$u_1 = \begin{cases} \frac{(y-0.3)\left((x-0.3)^2+(y-0.3)^2-0.01\right)}{\beta_1}, & \text{if } (x,y)^T \in \Omega_1 \\ \frac{(y-0.3)\left((x-0.3)^2+(y-0.3)^2-0.01\right)}{\beta_2}, & \text{if } (x,y)^T \in \Omega_2 \end{cases} \tag{63}$$

$$u_2 = \begin{cases} \frac{-(x-0.3)\left((x-0.3)^2+(y-0.3)^2-0.01\right)}{\beta_1}, & \text{if } (x,y)^T \in \Omega_1 \\ \frac{-(x-0.3)\left((x-0.3)^2+(y-0.3)^2-0.01\right)}{\beta_2}, & \text{if } (x,y)^T \in \Omega_2 \end{cases} \tag{64}$$

and

$$p = \frac{1}{10}\left(x^3 - y^3\right), \quad \forall (x,y)^T \in \Omega. \tag{65}$$

We solve (1)-(8) by virtue of the DLM/FD finite element method (37)-(40) to attain the numerical solutions $\boldsymbol{u}_h = (u_h, v_h)^T$ and p_h in the entire domain Ω, where the initial pressure is taken as zero. In order to implement the Algorithm (3.1), two partitions $T_h(\Omega)$ and $T_H(\Omega_2)$ are used, see e.g. Figure 3. We remark that $T_h(\Omega)$ and $T_H(\Omega_2)$ are constructed independently.

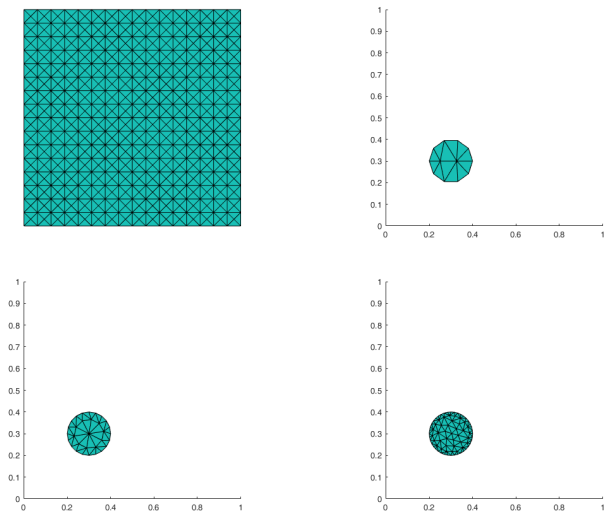

FIGURE 3. meshes: (a) $T_h(\Omega)$; (b) $T_H(\Omega_2)$ with $h = 1/8$; (c) $T_H(\Omega_2)$ with $h = 1/16$; (d) $T_H(\Omega_2)$ with $h = 1/32$.

Numerical approximation errors are reported in Tables 1 and 3 with the increasing jump of diffusion coefficients and different mesh ratios h/H. After conducting

a linear fitting over the approximation errors of different norms given in each table, we get numerical convergence rates as shown in those tables. We observe that when the jump ratio is small, say, $\beta_2/\beta_1 = 10$, there are not much difference on convergence errors and rates for the velocity in H^1, L^2 and L^∞ norms and the pressure in L^2 norm with different mesh ratios h/H from 1/2 to 2. However, when the jump ratio turns to large, the convergence errors and rates of all variables in different norms present large differences, and, the convergence rate of velocity in L^2 norm particularly approaches to the optimal (second order), as shown in cases of $\beta_2/\beta_1 = 100$ and 10000. In addition, we found out the mesh ratio $h/H = 1/2$ seems to produce a more satisfactory convergence result that matches with the predicted theoretical result for all jump ratios β_2/β_1, i.e., the first order optimal convergence rate for velocity in H^1 norm and the second order rate for pressure in L^2 norm for all jump ratios. Hence, we need to appropriately choose the mesh ratio in practice in order to make Lagrange multipliers work better.

Note the numerical results illustrated in Tables 4 and 5, the convergence errors of velocity in L^∞ norm present an optimal (second order) convergence rate for larger jump ratios under the mesh ratio $h/H = 1/2$, which is similar with the convergence rates of L^2 norm. This is not illustrated yet in the a priori error estimate result, an unusual result for the nonconforming IFE method that is used in this paper, because the original nonconforming IFE space does not have an optimal convergence rate in L^∞ norm due to the consistent error caused by the discontinuities of the test functions [not in $H^1(\Omega)$ space] [11]. Now our numerical experiments show that the newly developed DLM/FD-IFE method has $O(h^2)$ convergence for the velocity in L^∞ norm, which needs further theoretical investigation in our future work. Figures 4-6 illustrate the convergence rate of each case via a log-log plot.

TABLE 1. Results of Example 1, $\beta_2/\beta_1 = 10$.

h	H	$\|\|u-u_h\|\|_1$	$\|\|u-u_h\|\|_0$	$\|\|v-v_h\|\|_1$	$\|\|v-v_h\|\|_0$	$\|\|p-p_h\|\|_0$
1/16	1/8	1.4894e-02	2.2684e-04	1.4890e-02	2.2660e-04	6.1723e-03
1/32	1/16	7.3822e-03	6.0820e-05	7.3829e-03	6.0910e-05	1.4468e-03
1/64	1/32	3.6983e-03	2.9734e-05	3.6990e-03	2.9772e-05	2.8335e-04
rate		1.00	1.47	1.00	1.46	2.22
h	H	$\|\|u-u_h\|\|_1$	$\|\|u-u_h\|\|_0$	$\|\|v-v_h\|\|_1$	$\|\|v-v_h\|\|_0$	$\|\|p-p_h\|\|_0$
1/16	1/16	1.4900e-02	2.2454e-04	1.4901e-02	2.2460e-04	6.1026e-03
1/32	1/32	7.3995e-03	6.0315e-05	7.3959e-03	6.0289e-05	1.4262e-03
1/64	1/64	3.7030e-03	2.9245e-05	3.7032e-03	2.9283e-05	2.6893e-04
rate		1.00	1.47	1.00	1.47	2.25
h	H	$\|\|u-u_h\|\|_1$	$\|\|u-u_h\|\|_0$	$\|\|v-v_h\|\|_1$	$\|\|v-v_h\|\|_0$	$\|\|p-p_h\|\|_0$
1/16	1/32	1.4925e-02	2.2253e-04	1.4925e-02	2.2255e-04	6.1574e-03
1/32	1/64	7.4113e-03	5.9864e-05	7.4110e-03	5.9883e-05	1.4187e-03
1/64	1/128	3.7142e-03	2.8415e-05	3.7144e-03	2.8447e-05	2.8551e-04
rate		1.00	1.48	1.00	1.48	2.22

Another numerical phenomenon that is worthy to be pointed out is that the number of iteration in Algorithm 3.1 uniformly preserves a constant value, e.g., the iterative errors of Example 1 always converge down to the tolerance $\varepsilon = 10^{-6}$ within 2 steps no matter what kind of mesh ratios and jump ratios are used.

4.2. Example 2: Stokes/elliptic interface problems. The following functions $\boldsymbol{u} = (u_1, u_2)^T$ and p are chosen as the real solutions of (10) and (16) by properly

TABLE 2. Results of Example 1, $\beta_2/\beta_1 = 100$.

h	H	$\|\|u-u_h\|\|_1$	$\|\|u-u_h\|\|_0$	$\|\|v-v_h\|\|_1$	$\|\|v-v_h\|\|_0$	$\|\|p-p_h\|\|_0$
1/16	1/8	1.4913e-02	2.2767e-04	1.4913e-02	2.2744e-04	5.9470e-03
1/32	1/16	7.3878e-03	5.7882e-05	7.3887e-03	5.7870e-05	1.3487e-03
1/64	1/32	3.6839e-03	1.5561e-05	3.6849e-03	1.5609e-05	4.3442e-04
rate		1.01	1.94	1.01	1.93	1.89
h	H	$\|\|u-u_h\|\|_1$	$\|\|u-u_h\|\|_0$	$\|\|v-v_h\|\|_1$	$\|\|v-v_h\|\|_0$	$\|\|p-p_h\|\|_0$
1/16	1/16	1.4988e-02	2.3016e-04	1.4982e-02	2.2957e-04	5.9668e-03
1/32	1/32	7.4533e-03	6.3633e-05	7.4537e-03	6.3718e-05	1.4314e-03
1/64	1/64	3.7194e-03	1.8742e-05	3.7202e-03	1.8868e-05	5.2417e-04
rate		1.01	1.81	1.00	1.80	1.75
h	H	$\|\|u-u_h\|\|_1$	$\|\|u-u_h\|\|_0$	$\|\|v-v_h\|\|_1$	$\|\|v-v_h\|\|_0$	$\|\|p-p_h\|\|_0$
1/16	1/32	1.5145e-02	2.4292e-04	1.5155e-02	2.4396e-04	6.5127e-03
1/32	1/64	7.4966e-03	6.8739e-05	7.4973e-03	6.8789e-05	1.4037e-03
1/64	1/128	3.7510e-03	2.1750e-05	3.7517e-03	2.1800e-05	5.9651e-04
rate		1.01	1.74	1.01	1.74	1.72

TABLE 3. Results of Example 1, $\beta_2/\beta_1 = 10000$.

h	H	$\|\|u-u_h\|\|_1$	$\|\|u-u_h\|\|_0$	$\|\|v-v_h\|\|_1$	$\|\|v-v_h\|\|_0$	$\|\|p-p_h\|\|_0$
1/16	1/8	1.4918e-02	2.2842e-04	1.4920e-02	2.2831e-04	5.9306e-03
1/32	1/16	7.3913e-03	5.8920e-05	7.3923e-03	5.8907e-05	1.3436e-03
1/64	1/32	3.6864e-03	1.6766e-05	3.6873e-03	1.6837e-05	4.7432e-04
rate		1.01	1.88	1.01	1.88	1.82
h	H	$\|\|u-u_h\|\|_1$	$\|\|u-u_h\|\|_0$	$\|\|v-v_h\|\|_1$	$\|\|v-v_h\|\|_0$	$\|\|p-p_h\|\|_0$
1/16	1/16	1.5224e-02	2.5075e-04	1.5205e-02	2.4972e-04	6.7370e-03
1/32	1/32	7.4959e-03	6.9755e-05	7.5079e-03	7.1019e-05	1.5797e-03
1/64	1/64	3.7711e-03	2.5219e-05	3.7780e-03	2.5817e-05	6.5525e-04
rate		1.01	1.66	1.00	1.64	1.68
h	H	$\|\|u-u_h\|\|_1$	$\|\|u-u_h\|\|_0$	$\|\|v-v_h\|\|_1$	$\|\|v-v_h\|\|_0$	$\|\|p-p_h\|\|_0$
1/16	1/32	1.5365e-02	2.7168e-04	1.5368e-02	2.7189e-04	7.3529e-03
1/32	1/64	7.5716e-03	7.8890e-05	7.5719e-03	7.8910e-05	1.5869e-03
1/64	1/128	3.8333e-03	3.1365e-05	3.8339e-03	3.1416e-05	7.8793e-04
rate		1.00	1.56	1.00	1.56	1.61

TABLE 4. $||\tilde{\boldsymbol{u}} - \boldsymbol{u}_h||_\infty$ of Example 1, $\beta_2/\beta_1 = 100$.

h	H	$\|\|u-u_h\|\|_\infty$	$\|\|v-v_h\|\|_\infty$
1/16	1/8	1.0627e-03	1.0627e-03
1/32	1/16	2.6416e-04	2.6416e-04
1/64	1/32	6.7324e-05	6.7324e-05
rate		1.99	1.99

defining the right hand side functions $\boldsymbol{f}_1$, $\boldsymbol{f}_2$ and the jump flux function $\boldsymbol{w}$:

$$u_1 = \begin{cases} \frac{(y-0.3)\left((x-0.3)^2+(y-0.3)^2-0.01\right)}{\beta_1}, & \text{if } (x,y)^T \in \Omega_1 \\ \frac{(y-0.3)\left((x-0.3)^2+(y-0.3)^2-0.01\right)}{\beta_2}, & \text{if } (x,y)^T \in \Omega_2 \end{cases} \tag{66}$$

$$u_2 = \begin{cases} \frac{-(x-0.3)\left((x-0.3)^2+(y-0.3)^2-0.01\right)}{\beta_1}, & \text{if } (x,y)^T \in \Omega_1 \\ \frac{-(x-0.3)\left((x-0.3)^2+(y-0.3)^2-0.01\right)}{\beta_2}, & \text{if } (x,y)^T \in \Omega_2 \end{cases} \tag{67}$$

TABLE 5. $||\tilde{\boldsymbol{u}} - \boldsymbol{u}_h||_\infty$ of Example 1, $\beta_2/\beta_1 = 10000$.

h	H	$\|\|u - u_h\|\|_\infty$	$\|\|v - v_h\|\|_\infty$
1/16	1/8	1.0627e-03	1.0627e-03
1/32	1/16	2.6416e-04	2.6416e-04
1/64	1/32	8.2646e-05	8.0519e-05
rate		1.84	1.86

TABLE 6. Results of Example 2, $\beta_2/\beta_1 = 10$.

h	H	$\|\|u - u_h\|\|_1$	$\|\|u - u_h\|\|_0$	$\|\|v - v_h\|\|_1$	$\|\|v - v_h\|\|_0$	$\|\|p - p_h\|\|_0$
1/16	1/8	1.6193e-02	2.3147e-04	1.6191e-02	2.3136e-04	2.2083e-01
1/32	1/16	7.7074e-03	6.0737e-05	7.7081e-03	6.0816e-05	7.6777e-02
1/64	1/32	3.7637e-03	2.9484e-05	3.7644e-03	2.9500e-05	2.4746e-02
rate		1.05	1.49	1.05	1.49	1.58
h	H	$\|\|u - u_h\|\|_1$	$\|\|u - u_h\|\|_0$	$\|\|v - v_h\|\|_1$	$\|\|v - v_h\|\|_0$	$\|\|p - p_h\|\|_0$
1/16	1/16	1.6202e-02	2.2932e-04	1.6203e-02	2.2937e-04	2.2157e-01
1/32	1/32	7.7248e-03	6.0191e-05	7.7222e-03	6.0161e-05	7.6903e-02
1/64	1/64	3.7692e-03	2.8903e-05	3.7692e-03	2.8943e-05	2.4859e-02
rate		1.05	1.49	1.05	1.49	1.58
h	H	$\|\|u - u_h\|\|_1$	$\|\|u - u_h\|\|_0$	$\|\|v - v_h\|\|_1$	$\|\|v - v_h\|\|_0$	$\|\|p - p_h\|\|_0$
1/16	1/32	1.6225e-02	2.2770e-04	1.6225e-02	2.2769e-04	2.2246e-01
1/32	1/64	7.7362e-03	5.9699e-05	7.7359e-03	5.9719e-05	7.6786e-02
1/64	1/128	3.7803e-03	2.8072e-05	3.7805e-03	2.8107e-05	2.4751e-02
rate		1.05	1.51	1.05	1.51	1.58

TABLE 7. Results of Example 2, $\beta_2/\beta_1 = 100$.

h	H	$\|\|u - u_h\|\|_1$	$\|\|u - u_h\|\|_0$	$\|\|v - v_h\|\|_1$	$\|\|v - v_h\|\|_0$	$\|\|p - p_h\|\|_0$
1/16	1/8	1.6213e-02	2.3265e-04	1.6212e-02	2.3245e-04	2.2033e-01
1/32	1/16	7.7133e-03	5.7760e-05	7.7142e-03	5.7647e-05	7.6585e-02
1/64	1/32	3.7498e-03	1.5066e-05	3.7510e-03	1.5123e-05	2.4597e-02
rate		1.06	1.97	1.06	1.97	1.58
h	H	$\|\|u - u_h\|\|_1$	$\|\|u - u_h\|\|_0$	$\|\|v - v_h\|\|_1$	$\|\|v - v_h\|\|_0$	$\|\|p - p_h\|\|_0$
1/16	1/16	1.6288e-02	2.3548e-04	1.6286e-02	2.3503e-04	2.2324e-01
1/32	1/32	7.7785e-03	6.3861e-05	7.7793e-03	6.3863e-05	7.6634e-02
1/64	1/64	3.7854e-03	1.8306e-05	3.7863e-03	1.8445e-05	2.4529e-02
rate		1.05	1.84	1.05	1.84	1.59
h	H	$\|\|u - u_h\|\|_1$	$\|\|u - u_h\|\|_0$	$\|\|v - v_h\|\|_1$	$\|\|v - v_h\|\|_0$	$\|\|p - p_h\|\|_0$
1/16	1/32	1.6446e-02	2.4853e-04	1.6452e-02	2.4902e-04	2.2579e-01
1/32	1/64	7.8196e-03	6.8734e-05	7.8202e-03	6.8806e-05	7.6546e-02
1/64	1/128	3.8166e-03	2.1399e-05	3.8173e-03	2.1453e-05	2.4477e-02
rate		1.05	1.77	1.05	1.77	1.60

and

$$p = \frac{1}{10}\left(x^3 - y^3\right)\left((x-0.3)^2 + (y-0.3)^2 - 0.01\right), \quad \forall (x,y)^T \in \Omega_1. \tag{68}$$

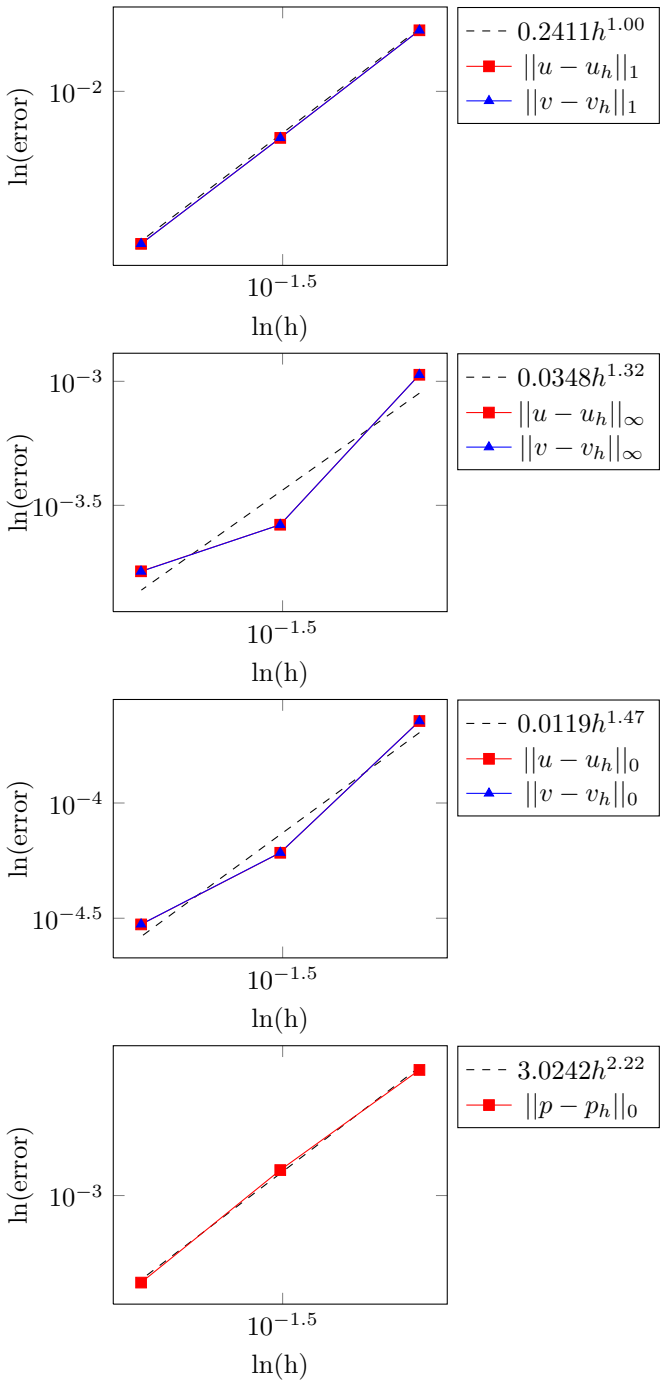

FIGURE 4. Log-log convergence plots of Example 1 ($\beta_2/\beta_1 = 10$, $h/H = 1/2$).

As shown in Tables 6-10, by applying the developed DLM/FD-IFE method to the aforementioned Stokes/elliptic interface model problem, we obtain similar numerical results with those of Example 1, i.e., the mesh ratio $h/H = 1/2$ produces

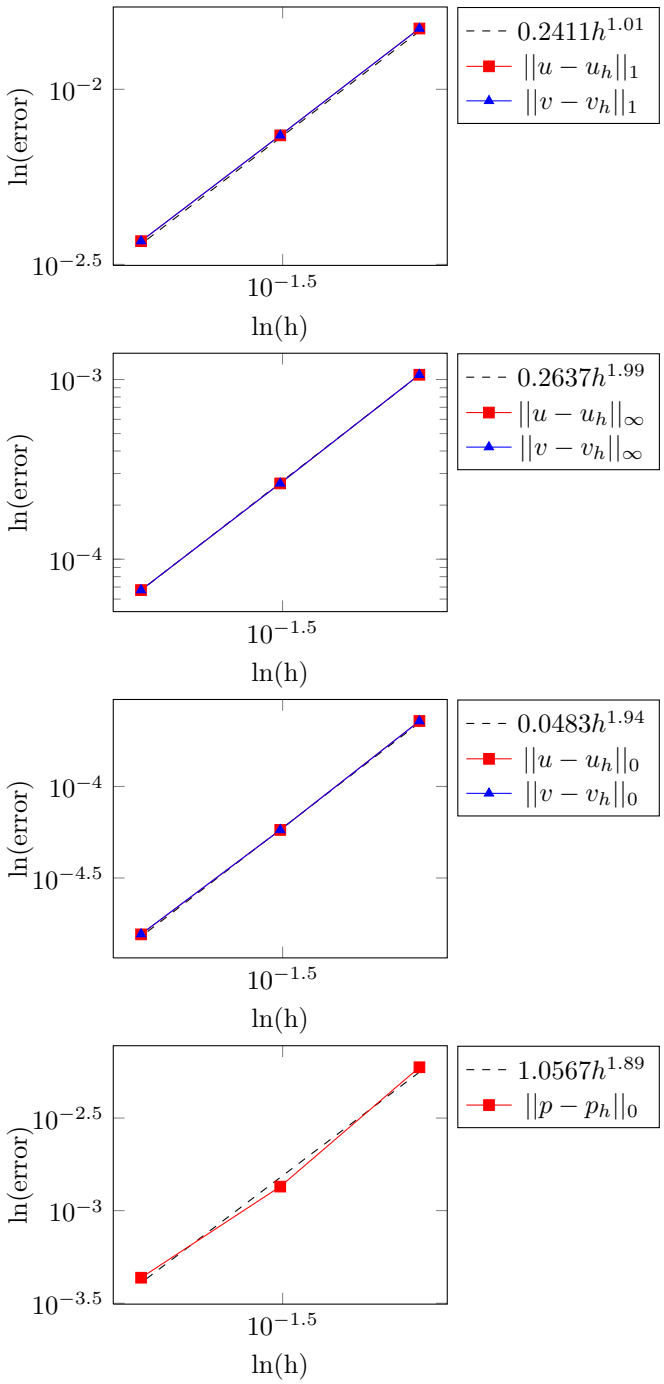

FIGURE 5. Log-log convergence plots of Example 1 ($\beta_2/\beta_1 = 100$, $h/H = 1/2$).

the best convergence for the velocity and the pressure, and when the jump ratio turns to large ($\beta_2/\beta_1 = 100, 10000$), it also results in the optimal error estimates for $\|\tilde{\boldsymbol{u}} - \boldsymbol{u}_h\|_{H^1(\Omega)}$ with the first order, and for $\|\tilde{\boldsymbol{u}} - \boldsymbol{u}_h\|_{L^2(\Omega)}$ and $\|\tilde{\boldsymbol{u}} - \boldsymbol{u}_h\|_{L^\infty(\Omega)}$

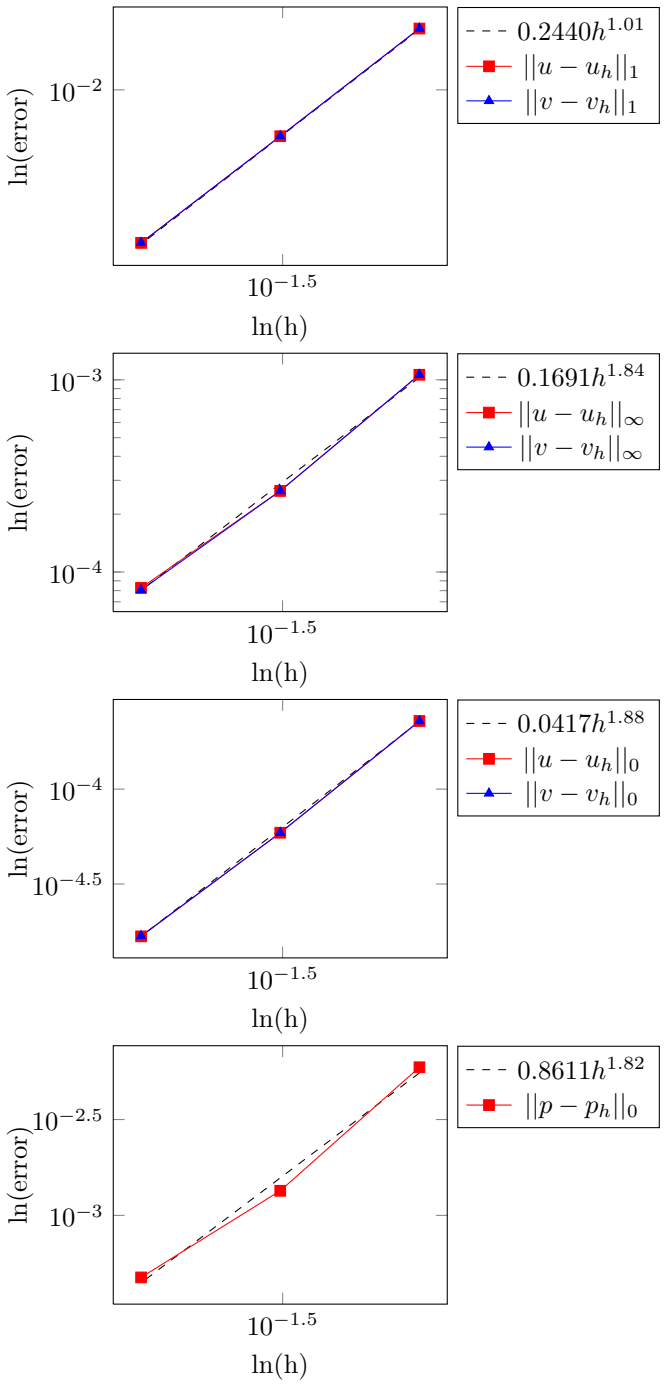

FIGURE 6. Log-log convergence plots of Example 1 ($\beta_2/\beta_1 = 10000$, $h/H = 1/2$).

with the second order, except for $\|\tilde{p} - p_h\|_{L^2(\Omega)}$ which shows the 1.5-th order convergence rate that is half order lower than that of Example 1. Figures 7-9 illustrate the convergence rate of each case via a log-log plot.

TABLE 8. Results of Example 2, $\beta_2/\beta_1 = 10000$.

h	H	$\|\|u-u_h\|\|_1$	$\|\|u-u_h\|\|_0$	$\|\|v-v_h\|\|_1$	$\|\|v-v_h\|\|_0$	$\|\|p-p_h\|\|_0$
1/16	1/8	1.6218e-02	2.3368e-04	1.6220e-02	2.3360e-04	2.2034e-01
1/32	1/16	7.7168e-03	5.8808e-05	7.7179e-03	5.8696e-05	7.6594e-02
1/64	1/32	3.7524e-03	1.6317e-05	3.7536e-03	1.6400e-05	2.4572e-02
rate		1.06	1.92	1.06	1.92	1.58
h	H	$\|\|u-u_h\|\|_1$	$\|\|u-u_h\|\|_0$	$\|\|v-v_h\|\|_1$	$\|\|v-v_h\|\|_0$	$\|\|p-p_h\|\|_0$
1/16	1/16	1.6545e-02	2.5997e-04	1.6530e-02	2.5900e-04	2.2834e-01
1/32	1/32	7.8219e-03	7.0301e-05	7.8311e-03	7.1221e-05	7.6500e-02
1/64	1/64	3.8367e-03	2.5087e-05	3.8436e-03	2.5680e-05	2.4492e-02
rate		1.05	1.69	1.05	1.67	1.61
h	H	$\|\|u-u_h\|\|_1$	$\|\|u-u_h\|\|_0$	$\|\|v-v_h\|\|_1$	$\|\|v-v_h\|\|_0$	$\|\|p-p_h\|\|_0$
1/16	1/32	1.6671e-02	2.7873e-04	1.6673e-02	2.7891e-04	2.2291e-01
1/32	1/64	7.8937e-03	7.9160e-05	7.8940e-03	7.9187e-05	7.6365e-02
1/64	1/128	3.8981e-03	3.1208e-05	3.8987e-03	3.1261e-05	2.4474e-02
rate		1.05	1.58	1.05	1.58	1.59

TABLE 9. $||\tilde{\boldsymbol{u}} - \tilde{\boldsymbol{u}}_h||_\infty$ of Example 2, $\beta_2/\beta_1 = 100$.

h	H	$\|\|u-u_h\|\|_\infty$	$\|\|v-v_h\|\|_\infty$
1/16	1/8	1.2167e-03	1.2167e-03
1/32	1/16	3.1165e-04	3.1165e-04
1/64	1/32	7.7848e-05	7.7848e-05
rate		1.98	1.98

TABLE 10. $||\tilde{\boldsymbol{u}} - \tilde{\boldsymbol{u}}_h||_\infty$ of Example 2, $\beta_2/\beta_1 = 10000$.

h	H	$\|\|u-u_h\|\|_\infty$	$\|\|v-v_h\|\|_\infty$
1/16	1/8	1.2166e-03	1.2167e-03
1/32	1/16	3.1165e-04	3.1165e-04
1/64	1/32	8.4471e-05	8.1778e-05
rate		1.93	1.94

In addition, same with Example 1, the number of iteration that is counted for Example 2 following Algorithm 3.6 is also uniform, preserving 2 iterations to reach the convergence tolerance $\varepsilon = 10^{-6}$, which is independent of mesh ratios and jump ratio.

5. Conclusion

By utilizing the original immersed finite element (IFE) space in the immersed elements, and designing an iterative construction approach based upon the jump flux interface condition which involves multiple primary variables, in this paper we develop a combined distributed Lagrange multiplier/fictitious domain–immersed finite element (DLM/FD-IFE) method to solve various interface problems with different interface conditions, including fluid-structure interaction problems which represent a large class of interface problems whose governing equations are different on either side of the interface. For the first time, we make the traditional IFE method which was originally designed for the elliptic interface problem now work

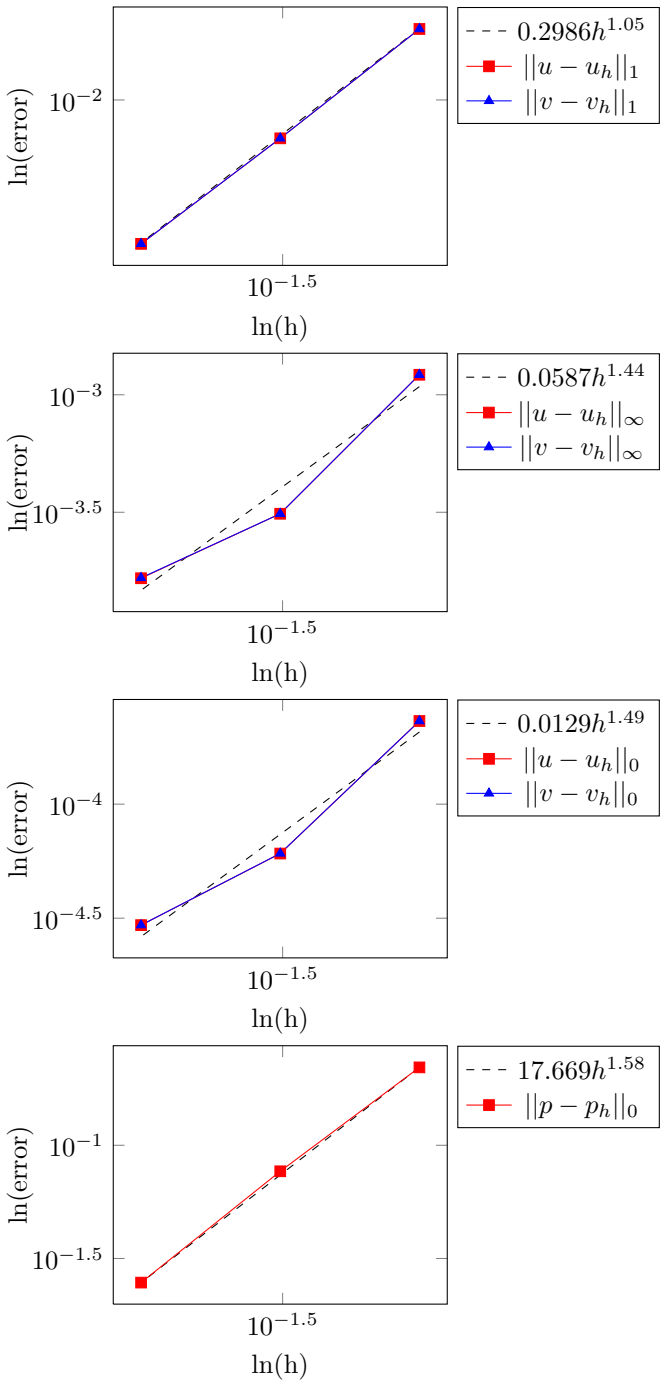

FIGURE 7. Log-log convergence plots of Example 2 ($\beta_2/\beta_2 = 10$, $h/H = 1/2$).

for more general interface problems without considering governing equations on both sides of the interface have to be identical.

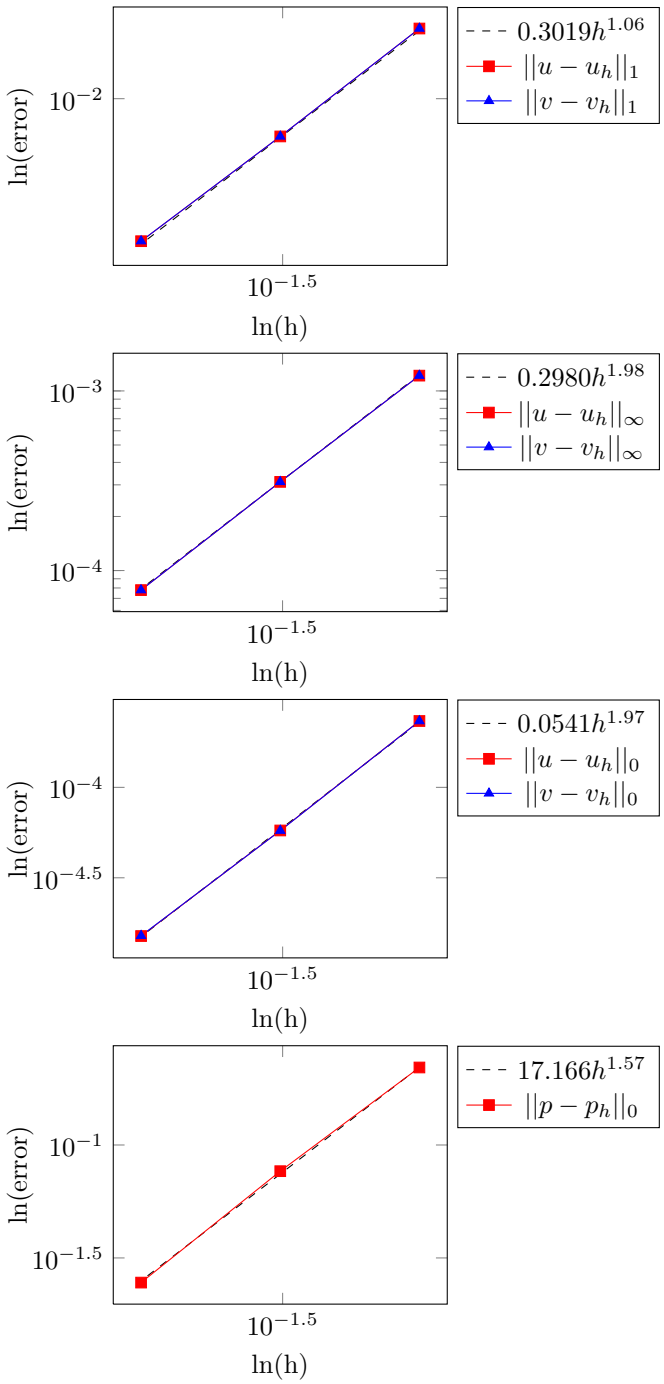

FIGURE 8. Log-log convergence plots of Example 2 ($\beta_2/\beta_1 = 100$, $h/H = 1/2$).

Stokes- and Stokes/elliptic interface problems are taken as examples in this paper to illustrate the strength of the developed DLM/FD-IFE method, where, the optimal convergence rates are obtained for the velocity in norms of H^1 (the first

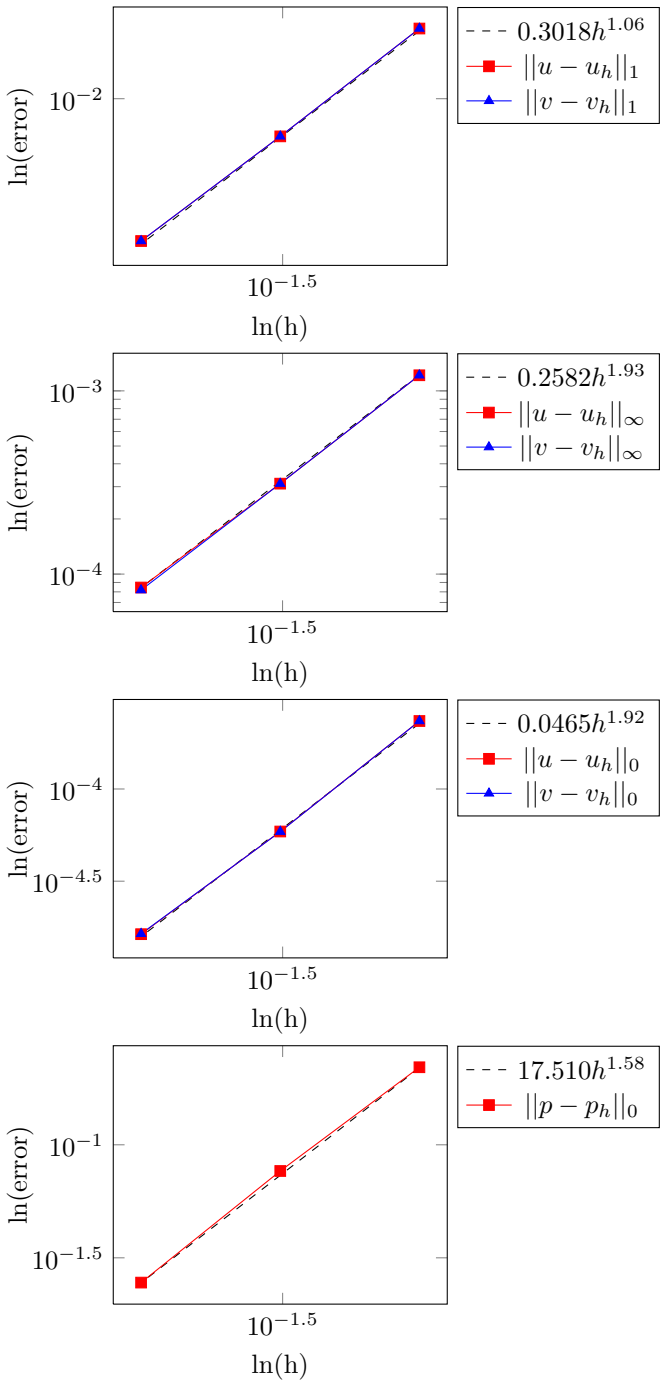

FIGURE 9. Log-log convergence plots of Example 2 ($\beta_2/\beta_1 = 10000$, $h/H = 1/2$).

order), L^2 (the second order) and L^∞ (the second order), and the 1.5-th up to the second order convergence for the pressure in L^2 norm under the mesh ratio $h/H = 1/2$ for large jump ratios $\beta_2/\beta_1 = 100$ and 10000. In these Stokes-involved

interface problems, the discretized pressure is taken as an iterative variable to iteratively construct the IFE space, and the number of iteration remains uniform which is independent of mesh ratios and jump ratios.

Acknowledgments

P. Sun was supported by NSF Grant DMS-1418806, Z. Li was supported by NSF grant DMS-1522768.

References

[1] S. Adjerid, M. Ben-Romdhane, and T. LIN. Higher degree immersed finite element methods for second-order elliptic interface problems. *International Journal of Numerical Analysis and Modeling*, 11:541–566.

[2] Slimane Adjerid, Nabil Chaabane, and Tao Lin. An immersed discontinuous finite element method for Stokes interface problems. *Computer Methods in Applied Mechanics and Engineering*, 293:170–190, 2015.

[3] F. Auricchio, D. Boffi, L. Gastaldi, A. Lefieux, and A. Reali. On a fictitious domain method with distributed Lagrange multiplier for interface problems. *Applied Numerical Mathematics*, 95:36 – 50, 2015.

[4] F. Auricchio, D. Boffi, L. Gastaldi, A. Lefieux, and A. Reali. On a fictitious domain method with distributed Lagrange multiplier for interface problems. *Applied Numerical Mathematics*, 95:36–50, 2015.

[5] Ivo Babuška. Error-bounds for finite element method. *Numerische Mathematik*, 16(4):322–333, 1971.

[6] D. Boffi and L. Gastaldi. A fictitious domain approach with Lagrange multiplier for fluid-structure interactions. *Numer. Math.*, pages DOI 10.1007/s00211–016–0814–1, 2016 (in press).

[7] D. Boffi, L. Gastaldi, and M. Ruggeri. Mixed formulation for interface problems with distributed lagrange multiplier. *Computers & Mathematics with Applications*, 68:2151 – 2166, 2014.

[8] D. Boffi, L. Gastaldi, and M. Ruggeri. Mixed formulation for interface problems with distributed Lagrange multiplier. *Computers & Mathematics with Applications*, 68(12, Part B):2151 – 2166, 2014.

[9] F. Brezzi. On the existence, uniqueness and approximation of saddle point problems arising from Lagrangian multipliers. *RAIRO Analyse Numerique*, 8:129–151, 1974.

[10] S. K. Chakrabarti, editor. *Numerical Models in Fluid Structure Interaction, Advances in Fluid Mechanics*, volume 42. WIT Press, 2005.

[11] S. Chou, D. Kwak, and K. Wee. Optimal convergence analysis of an immersed interface finite element method. *Adv. Comput. Math.*, 33:149–168, 2010.

[12] E. H. Dowell and K. C. Hall. Modeling of fluid-structure interaction. *Annu. Rev. Fluid Mech.*, 33:445–490, 2001.

[13] R. Glowinski, T.W. Pan, T.I. Hesla, and D.D. Joseph. A distributed Lagrange multiplier/fictitious domain method for particulate flows. *International Journal of Multiphase Flow*, 25(5):755 – 794, 1999.

[14] R. Glowinski, T.W. Pan, T.I. Hesla, D.D. Joseph, and J. Périaux. A fictitious domain approach to the direct numerical simulation of incompressible viscous flow past moving rigid bodies: Application to particulate flow. *Journal of Computational Physics*, 169(2):363 – 426, 2001.

[15] A. Hansbo and P. Hansbo. An unfitted finite element method, based on Nitsche's method, for elliptic interface problems. *Comput. Methods Appl. Mech. Engrg.*, 191:5537–5552, 2002.

[16] X. He, T. Lin, and Y. Lin. Immersed finite element methods for elliptic interface problems with non-homogeneous jump conditions. *International Journal of Numerical Analysis and Modeling*, 8:284–301, 2011.

[17] X. He, T. Lin, and Y. Lin. A selective immersed discontinuous galerkin method for elliptic interface problems. *Mathematical Methods in the Applied Sciences*, 37:983–1002, 2014.

[18] H. Ji, J. Chen, and Z. Li. A symmetric and consistent immersed finite element method for interface problems. *Journal of Scientific Computing*, 61:533–557, 2014.

[19] H. Ji, J. Chen, and Z. Li. A new augmented immersed finite element method without using svd interpolations. *Numerical Algorithms*, 71:395–416, 2016.

[20] R.J. LeVeque and Z. Li. The immersed interface method for elliptic equations with discontinuous coefficients and singular sources. *SIAM J. Numer. Anal.*, 31:1019–1044, 1994.
[21] Z. Li. The immersed interface method using a finite element formulation. *Applied Numer. Math.*, 27:253–267, 1998.
[22] Z. Li. An augmented Cartesian grid method for Stokes-Darcy fluid-structure interactions, 2015.
[23] Z. Li, T. Lin, Y. Lin, and R. C. Rogers. An immersed finite element space and its approximation capability. *Numerical Methods for Partial Differential Equations*, 20:338–367, 2004.
[24] Z. Li, L. Xi, Q. Cai, H. Zhao, and R. Luo. A semi-implicit augmented IIM for Navier-Stokes equations with open and traction boundary conditions. *Journal of Computational Physics*, 297:182–193, 2015.
[25] X. Liu and S. Li. A variational multiscale stabilized finite element method for the stokes flow problem. *Finite Elements in Analysis and Design*, 42:580 – 591, 2006.
[26] A. Lundberg, P. Sun, and C. Wang. Distributed Lagrange multiplier-fictitious domain finite element method for Stokes interface problems. *Comput. Math. Appl.*, 2017 (submitted).
[27] R. Massjung. An unfitted discontinuous Galerkin method applied to elliptic interface problems. 50:3134–3162, 2012.
[28] H. J.-P Morand and R. Ohayon. *Fluid-Structure Interaction: Applied Numerical Methods*, volume 42. Wiley, 1995.
[29] S. Nicaise. *Polygonal Interface Problems*, volume 39 of *Methoden und Verfahren der Mathematischen Physik (Methods and Procedures in Mathematical Physics)*. Verlag Peter D. Lang, Frankfurt am Main, 1993.
[30] X. Shi and N. Phan-Thien. Distributed Lagrange multiplier/fictitious domain method in the framework of lattice boltzmann method for fluid-structure interactions. *J. Comput. Phys.*, 206:81–94, 2005.
[31] Y. Shibata and S. Shimizu. On a resolvent estimate of the interface problem for the Stokes system in a bounded domain. *Journal of Differential Equations*, 191(2):408 – 444, 2003.
[32] N. Sukumar, D. L. Chopp, and B. Moran. Extended finite element for three-dimensional fatigue crack propagation. *Engineering Fracture Mechanics*, 70:29–48, 2003.
[33] P. Sun. Fictitious domain finite element method for Stokes/elliptic interface problems with jump coefficients. *Appl Math Comput.*, 2017 (submitted).
[34] P. Sun and C. Wang. Fictitious domain finite element method for Stokes/parabolic interface problems with jump coefficients. *Appl. Numer. Math.*, 2018.
[35] C. Wang and P. Sun. A fictitious domain method with distributed Lagrange multiplier for parabolic problems with moving interfaces. *Journal of Scientific Computing*, doi=10.1007/s10915-016-0262-1, 2016.
[36] Z. Yu. A DLM/FD method for fluid/flexible-body interactions. *Journal of Computational Physics*, 207(1):1 – 27, 2005.
[37] Z. Yu, N. Phan-Thien, and R.I. Tanner. Dynamic simulation of sphere motion in a vertical tube. *J. Fluid Mech.*, 518:61–93, 2004.

School of Mathematical Sciences, Tongji University, Shanghai 200092, China
E-mail: wangcheng@tongji.edu.cn

Department of Mathematical Sciences, University of Nevada, Las Vegas, 4505 Maryland Parkway, Las Vegas, Nevada 89154, USA
E-mail, Corresponding author: pengtao.sun@unlv.edu

Department of Mathematics, North Carolina State University, Raleigh, NC 27695, USA
E-mail: zhilin@ncsu.edu